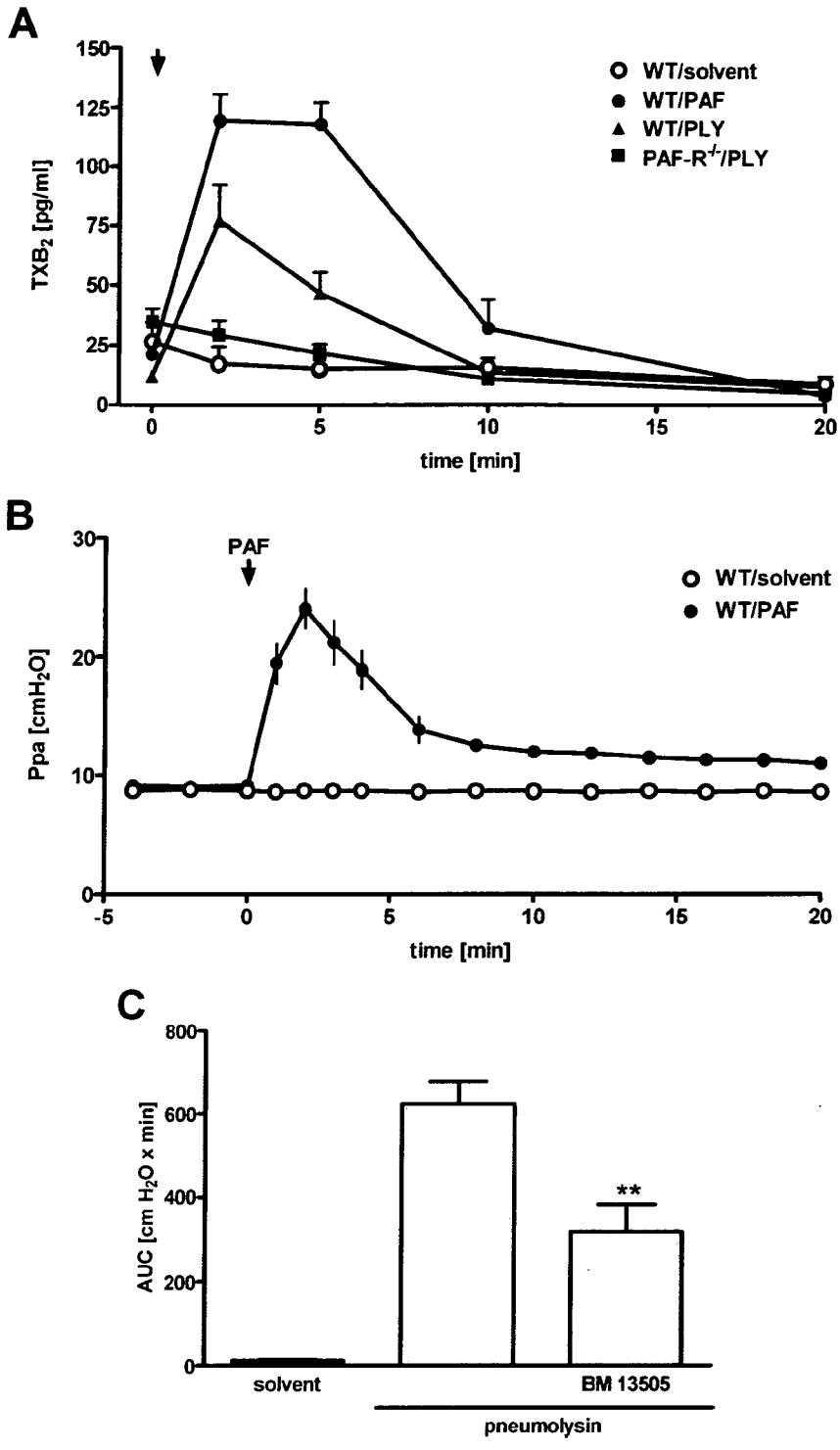

Figure 4. Pulmonary hypertension evoked by pneumolysin or platelet-activating factor (*PAF*) is partly mediated by thromboxane (*TXA_2*). *A*, TXB_2, a stable degradation product of TXA_2, was quantified in perfusion buffer sampled before and at 2, 5, 10, or 20 mins after pneumolysin (*PLY*) infusion (1 μg/min) in wild-type (*WT*) or PAF receptor–deficient (*PAF-$R^{-/-}$*) mice, or after PAF infusion (100 nM) in WT mice, respectively. PLY or PAF were infused for 1 min. *B*, pressure increases after PLY (1 μg/min) or PAF (100 nM) perfusion for 1 min are shown. *C*, the area under the pulmonary arterial pressure (*Ppa*) curve (*AUC*) values were reduced in PLY-challenged WT lungs preperfused with TXA_2 receptor antagonist BM 13505 (10 μM) compared with PLY-challenged WT lungs without BM 13505. $^{**}p < .01$ vs. WT/PLY.

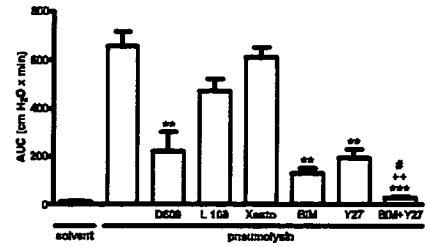

Figure 5. The pneumolysin-evoked pulmonary arterial pressure increase, as expressed by the area under the curve (*AUC*), was reduced in lungs preperfused with the phosphatidylcholine-specific phospholipase C inhibitor D 609 (100 μM) or with the protein kinase C inhibitor bisindolylmaleimide (*BIM*) (10 μM). The specific Rho-kinase inhibitor Y-27632 (*Y27*; 5 μM) also diminished the pulmonary arterial pressure increase, and the combination of BIM and Y-27632 showed additive effects. Inhibition of phosphatidylinositol-specific phospholipase C with L 108 (30 μM) or employment of the inositol trisphosphate receptor antagonist xestospongin C (*Xesto*; 10 μM) had no significant effect on pneumolysin-induced pulmonary hypertension. $^{**}p < .01$ vs. PLY; $^{***}p < .001$ vs. PLY; $\#p < .05$ vs. PLY/BIM; $++p < .01$ vs. PLY/Y27.

sion and to aerosolized PLY was decreased in lungs of PAF-$R^{-/-}$ mice.

DISCUSSION

The current study provides evidence that PLY-induced pulmonary hypertension and microvascular leakage is mediated by PAF. Isolated mouse lungs perfused with PLY responded with a rapid, dose-dependent increase of pulmonary vascular resistance, and increased amounts of PAF were measured in the tissue. Lungs of PAF-$R^{-/-}$ mice, and lungs of WT mice pretreated with a specific PAF-R antagonist, showed markedly reduced pressor responses. Both PLY- and exogenous PAF-induced hemodynamic alterations were accompanied by increased TXA_2 generation, and antagonism of the TXA_2 receptor diminished PLY-induced hypertension. Examination of downstream intracellular signaling pathways suggested major contributions of phosphatidylcholine-specific PLC and PKC and of the Rho-kinase pathway in PLY-induced pulmonary hypertension.

Several species of bacteria within the genera *Streptococcus*, *Clostridium*, *Bacillus*, and *Listeria* secrete cytolytic proteins that belong to the single, highly homologous family of thiol-activated, cholesterol-binding cytolysins. For lysation of cytoplasmic membranes, they require membrane cholesterol but no spe-

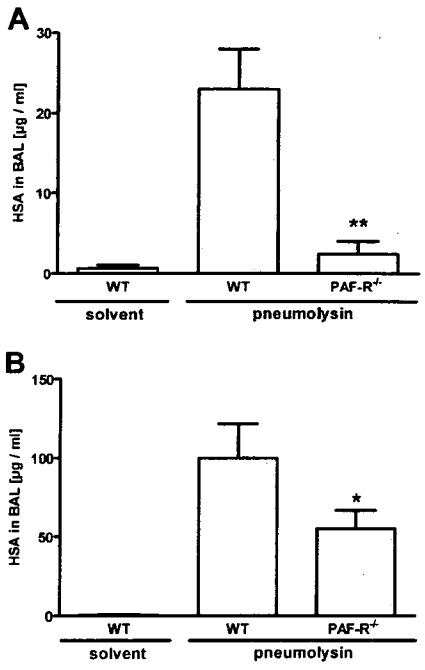

Figure 6. Pneumolysin-induced permeability was reduced in lungs of platelet-activating factor receptor deficient mice (*PAF-R*$^{-/-}$). Lungs were perfused with 0.04% human serum albumin (*HSA*). *A*, 1.0 µg/mL pneumolysin was infused for 1 min; *B*, 1.0 µg pneumolysin was aerosolized intratracheally. After 30 mins, bronchoalveolar lavage (*BAL*) was performed, and HSA was measured in BAL fluid. Pneumolysin evoked vascular leakage, as indicated by increased HSA concentration. *WT*, wild-type mice. $^{**}p < .01$ vs. WT/PLY; $^{*}p < .05$ vs. WT/PLY.

cific receptor (19). As a member of this family, PLY is an important virulence factor in pneumococcal disease, including pneumonia and sepsis (3, 4, 20–22), which is produced by all clinical isolates of *S. pneumoniae*. PLY-induced pore formation and cell lysation may be regarded as nonspecific, as compared with other members of this toxin family, but proinflammatory activities of PLY are important for the pathology of lung disease as well (23, 24). Correspondingly, PLY was a significant contributor to mortality in murine pneumococcal bacteremia (5) and sepsis (6). Purified PLY was capable of inducing major features of acute respiratory distress syndrome, including microvascular leakage and pulmonary hypertension, as we recently reported (7). In that study, endothelial localization of the toxin was noted in pulmonary arteries and in alveolar septs, and pulmonary arteries showing PLY immunostaining were exceedingly constricted. In contrast to WT PLY, Pd-B, a modified PLY with a single amino acid substitution at residue number 433 in the protein sequence (14), had no effect on Ppa in the present study, suggesting that the conserved undecapeptide sequence of PLY was responsible for vasoconstriction.

Addressing the mechanisms underlying the impressive PLY-induced lung damage, we employed ventilated, buffer-perfused mouse lungs. The model allows for measurement of fluid balance and real-time monitoring of lung hemodynamics on an intact organ level, independently from systemic inflammatory responses. In the current study, we did not focus on a potential role of blood components or recirculation phenomena.

The pulmonary PLY concentration in human pneumococcal pneumonia is not known. However, the PLY concentrations used in our study are in all probability realistic. Spreer et al. (25) observed that PLY levels in the cerebrospinal fluid during meningitis may reach 0.2 µg/mL, which is in the concentration range employed in our experiments. Moreover, in an intact mice model, we detected approximately 1×10^8 colony-forming units of *S. pneumoniae* in the lungs 6 hrs after infection, in parallel with significant lung injury (7). We do not exactly know the amount of PLY released from the pneumococci (NCTC 7978) in these *in vivo* experiments. However, *in vitro*, 1×10^8 of pneumococci of the same strain displayed a total hemolytic activity comparable with the hemolytic activity of 1.25 µg of recombinant PLY. Approximately 10% to 20% of the pneumococcal hemolytic activity were detected in the supernatant of bacterial cultures, which corresponds to the concentration range of recombinant PLY employed in our experiments. Thus, the PLY doses administered to the isolated perfused mice lungs may favorably compare with the PLY concentration in lungs of intact mice after infection with *S. pneumoniae*.

In endotoxin-induced acute lung inflammation, resident alveolar macrophages have been demonstrated to contribute to acute lung injury (26). Interestingly, early onset lung damage in intact mice challenged with PLY via the airways was independent of resident alveolar macrophages and newly recruited neutrophils and monocytes, suggesting direct pneumotoxicity of PLY (27). In line with these findings, we have recently demonstrated in a mouse model of pneumococcal pneumonia considerable lung microvascular leakage, which had already emerged at 6 hrs after transnasal infection. Significant neutrophil lung infiltration was not present at that point of time (7), suggesting that PLY substantially contributes to these early alterations. Therefore, the absence of circulating polymorphonuclear neutrophils and monocytes in our buffer-perfused lung model obviously does not play a major role for the rapid induction of severe lung damage by PLY.

Pneumococci firmly adhere to endothelial cells (28), and PLY released by these adherent pneumococci may thus directly affect the endothelium. Pulmonary endothelial cells synthesize and store several vasoactive mediators, including the proinflammatory phospholipid PAF (10, 29). Exotoxins of other pathogens, including *Escherichia coli* hemolysin and *Staphylococcus aureus* alpha-toxin, have been reported from our group to enhance PAF synthesis in endothelial cells (30, 31), and high PAF levels were detected in rat lungs after injection of lipopolysaccharide, mediating hemodynamic changes (32). Exogenous PAF potently contracted pulmonary vascular smooth muscle, causing pulmonary hypertension in rabbit and rat lungs (33, 34). Interestingly, PAF-R$^{-/-}$ mice had markedly reduced mortality in pneumococcal pneumonia (35) due to improved antibacterial host defense; however, pulmonary hemodynamics and lung injury were not examined in detail (35). We observed that perfusion of lungs with PLY resulted in increased PAF contents in the whole organ tissue. PAF synthesized by stimulated endothelial cells is not released into solution but almost completely remains cell associated (36), which may explain why PAF was not detectable in venous buffer effluate, despite increased tissue synthesis. Further evidence for an important role of PAF in PLY-induced pulmonary hypertension was provided by experiments employing lungs of PAF-R$^{-/-}$ mice, as these showed markedly reduced pressor responses compared with lungs of WT mice. In line with these findings, perfusion of lungs with the specific PAF-R antagonist BN 50730 before PLY infusion significantly decreased these pressor responses.

In isolated rabbit lungs, a thromboxane receptor antagonist diminished the pulmonary pressor response to PAF (34), and in rat lungs, PAF-induced smooth muscle contraction was largely mediated by thromboxane (TXA_2) and, to a smaller degree, by leukotrienes (37). In our model, intravascular PLY and exogenous PAF increased both Ppa and the content

of TXB_2, a stable degradation product of TXA_2, in the venous buffer effluate. Moreover, preperfusion with the thromboxane receptor antagonist BM 13505 distinctly reduced the PLY-induced pressor response in isolated mouse lungs. Some reduction was observed after lipoxygenase inhibition with AA-861 as well.

TXA_2 binds to the Gq-coupled thromboxane receptor. Gq-coupled receptors may activate 1) phosphatidylinositol-specific PLC (38), thereby increasing cytosolic IP_3 (38), and 2) phosphatidylcholine-specific PLC, resulting in diacylglycerol production. IP_3 induces cytosolic Ca^{2+} increase, followed by myosin light chain phosphorylation and subsequent smooth muscle contraction (38). Diacylglycerol activates PKC, leading to increased myosin light chain phosphorylation via diverse mechanisms (38). By using specific inhibitors, we demonstrated that the Ppa response to PLY in murine lungs depended primarily on phosphatidylcholine-specific PLC, but not phosphatidylinositol-specific PLC. Moreover, PLY-induced pressor responses were diminished after PKC inhibition but not altered by the potent IP_3-receptor antagonist xestospongin C. Consistent with these observations, xestospongin C failed to affect initial vasoconstriction to the thromboxane receptor agonist U46619 in perfused rat lungs (33). The concentration of xestospongin C employed in our experiments was three-fold above the median inhibitory concentration (39). Notably, at this concentration, xestospongin C prevented acetylcholine-induced calcium signaling in mouse lung slices (40) and attenuated PAF-induced edema formation in isolated rat lungs (41). Beyond IP_3 and PKC, activated Rho-kinase indirectly increases myosin light chain phosphorylation, thereby contributing to additional contractile force of myofilaments at fixed Ca^{2+} concentrations (42). Pretreatment with the Rho-kinase inhibitor Y-27632 (42) reduced the pressor response to PLY significantly. Although Y-27632 has been reported to alter TXA_2 generation in a recent study (33), the same work demonstrated extensive reduction of U46619-induced vasoconstriction by Rho-kinase inhibition in rat lungs (33), underscoring the importance of Rho-kinase in intracellular signal transduction subsequent to thromboxane receptor activation. In line with our results, this study further suggested a major role for Rho-kinase and found no contribution of the phosphatidylinositol-specific PLC and IP_3-dependent pathway in PAF- and TXA_2-induced pulmonary vasoconstriction (33).

The mechanism responsible for the residual pressor responses in PAF-$R^{-/-}$ mice remains speculative. Of note, combined PKC and Rho-kinase inhibition almost completely abolished the PLY-induced Ppa increases, underscoring the contribution of either pathway to PLY-induced pulmonary hypertension. Interestingly, a recent study demonstrated that sublytic concentrations of PLY produced rapid activation of Rho and Rac guanosine triphosphatases in neuroblastoma cells (43). However, a role of thromboxane-independent Rho-kinase activation by PLY in the lung has still to be defined.

In addition to pulmonary hypertension, microvascular leakage is an important feature of acute lung injury. We observed distinctly reduced permeability in lungs of PAF-$R^{-/-}$ mice stimulated with intravascular or aerosolized PLY. Notably, this reduction was not solely attributable to the decreased pressor response, as *aerosolized* PLY increased permeability without altering hemodynamics. As recently demonstrated, PAF-induced alterations in pulmonary vascular permeability are mediated by simultaneous activation of cyclooxygenase and acid sphingomyelinase, followed by subsequent production of prostaglandin E_2 and ceramide (44, 45). The contribution of these mechanisms to PLY-induced hyperpermeability requires further studies.

The implication of PAF in pulmonary disease has been clearly demonstrated in a variety of animal models, as recently reviewed (8). In humans, increased PAF levels have been found in pneumonia (46), acute respiratory distress syndrome (47), and sepsis (48, 49). However, there is only limited information on signaling pathways responsible for the responses to PAF in human tissue: PAF inhalation stimulated leukotriene and TXA_2 production in humans (50), and PAF activated PKC in human umbilical cord vein endothelial cells (51) and human epidermoid carcinoma cells (52) and activated Rho family proteins in human monocytic leukemia cells (53). These studies denote that a potential involvement of PAF in human pneumococcal pneumonia may include similar mechanisms as shown in our murine study.

In summary, our findings demonstrate a key role for PAF in PLY-induced pulmonary hypertension and microvascular leakage in mice, which are both hallmarks of acute lung injury. The PAF-R and its downstream signaling pathways may thus provide perspectives for specific pharmacologic interventions in pneumococci-evoked acute respiratory failure.

ACKNOWLEDGMENTS

We thank C. Thureau for BN 50730, A. C. Hocke for thoughtful discussions, and S. Preising, J. Thiele, and J. Ott for their skillful technical assistance.

REFERENCES

1. Ware LB, Matthay MA: The acute respiratory distress syndrome. *N Engl J Med* 2000; 342: 1334–1349
2. File TM: Community-acquired pneumonia. *Lancet* 2003; 362:1991–2001
3. Jedrzejas MJ: Pneumococcal virulence factors: Structure and function. *Microbiol Mol Biol Rev* 2001; 65:187–207
4. Mitchell TJ: Virulence factors and the pathogenesis of disease caused by *Streptococcus pneumoniae*. *Res Microbiol* 2000; 151: 413–419
5. Musher DM, Phan HM, Baughn RE: Protection against bacteremic pneumococcal infection by antibody to pneumolysin. *J Infect Dis* 2001; 183:827–830
6. Benton KA, Everson MP, Briles DE: A pneumolysin-negative mutant of *Streptococcus pneumoniae* causes chronic bacteremia rather than acute sepsis in mice. *Infect Immun* 1995; 63:448–455
7. Witzenrath M, Gutbier B, Hocke AC, et al: Role of pneumolysin for the development of acute lung injury in pneumococcal pneumonia. *Crit Care Med* 2006; 34:1947–1954
8. Uhlig S, Goggel R, Engel S: Mechanisms of platelet-activating factor (PAF)-mediated responses in the lung. *Pharmacol Rep* 2005; 57(Suppl):206–221
9. Wang H, Tan X, Chang H, et al: Regulation of platelet-activating factor receptor gene expression in vivo by endotoxin, platelet-activating factor and endogenous tumour necrosis factor. *Biochem J* 1997; 322:603–608
10. Prescott SM, Zimmerman GA, Stafforini DM, et al: Platelet-activating factor and related lipid mediators. *Annu Rev Biochem* 2000; 69:419–445
11. Ishii S, Kuwaki T, Nagase T, et al: Impaired anaphylactic responses with intact sensitivity to endotoxin in mice lacking a platelet-activating factor receptor. *J Exp Med* 1998; 187:1779–1788
12. von Bethmann AN, Brasch F, Nusing R, et al: Hyperventilation induces release of cytokines from perfused mouse lung. *Am J Respir Crit Care Med* 1998; 157:263–272
13. Paton JC, Andrew PW, Boulnois GJ, et al: Molecular analysis of the pathogenicity of *Streptococcus pneumoniae*: The role of pneumococcal proteins. *Annu Rev Microbiol* 1993; 47:89–115

14. Paton JC, Lock RA, Lee CJ, et al: Purification and immunogenicity of genetically obtained pneumolysin toxoids and their conjugation to *Streptococcus pneumoniae* type 19F polysaccharide. *Infect Immun* 1991; 59: 2297–2304
15. Seybold J, Thomas D, Witzenrath M, et al: Tumor necrosis factor-alpha-dependent expression of phosphodiesterase 2: Role in endothelial hyperpermeability. *Blood* 2005; 105:3569–3576
16. Owen JS, Wykle RL, Samuel MP, et al: An improved assay for platelet-activating factor using HPLC-tandem mass spectrometry. *J Lipid Res* 2005; 46:373–382
17. Lowry OH, Rosebrough NJ, Farr AL, et al: Protein measurement with the Folin phenol reagent. *J Biol Chem* 1951; 193:265–275
18. Clay KL: Quantitation of platelet-activating factor by gas chromatography-mass spectrometry. *Methods Enzymol* 1990; 187: 134–142
19. Palmer M: The family of thiol-activated, cholesterol-binding cytolysins. *Toxicon* 2001; 39:1681–1689
20. Cockeran R, Anderson R, Feldman C: The role of pneumolysin in the pathogenesis of *Streptococcus pneumoniae* infection. *Curr Opin Infect Dis* 2002; 15:235–239
21. Hirst RA, Kadioglu A, O'Callaghan C, et al: The role of pneumolysin in pneumococcal pneumonia and meningitis. *Clin Exp Immunol* 2004; 138:195–201
22. Paton JC: The contribution of pneumolysin to the pathogenicity of *Streptococcus pneumoniae*. *Trends Microbiol* 1996; 4:103–106
23. Rubins JB, Charboneau D, Fasching C, et al: Distinct roles for pneumolysin's cytotoxic and complement activities in the pathogenesis of pneumococcal pneumonia. *Am J Respir Crit Care Med* 1996; 153:1339–1346
24. Jounblat R, Kadioglu A, Mitchell TJ, et al: Pneumococcal behavior and host responses during bronchopneumonia are affected differently by the cytolytic and complement-activating activities of pneumolysin. *Infect Immun* 2003; 71:1813–1819
25. Spreer A, Lis A, Gerber J, et al: Differences in clinical manifestation of *Streptococcus pneumoniae* infection are not correlated with in vitro production and release of the virulence factors pneumolysin and lipoteichoic and teichoic acids. *J Clin Microbiol* 2004; 42:3342–3345
26. Maus UA, Koay MA, Delbeck T, et al: Role of resident alveolar macrophages in leukocyte traffic into the alveolar air space of intact mice. *Am J Physiol Lung Cell Mol Physiol* 2002; 282:L1245–L1252
27. Maus UA, Srivastava M, Paton JC, et al: Pneumolysin-induced lung injury is independent of leukocyte trafficking into the alveolar space. *J Immunol* 2004; 173:1307–1312
28. Cundell DR, Gerard NP, Gerard C, et al: *Streptococcus pneumoniae* anchor to activated human cells by the receptor for platelet-activating factor. *Nature* 1995; 377:435–438
29. Prescott SM, Zimmerman GA, McIntyre TM: Human endothelial cells in culture produce platelet-activating factor (1-alkyl-2-acetyl-sn-glycero-3-phosphocholine) when stimulated with thrombin. *Proc Nat Acad Sci U S A* 1984; 81:3534–3538
30. Krull M, Dold C, Hippenstiel S, et al: *Escherichia coli* hemolysin and *Staphylococcus aureus* alpha-toxin potently induce neutrophil adhesion to cultured human endothelial cells. *J Immunol* 1996; 157:4133–4140
31. Suttorp N, Buerke M, Tannert-Otto S: Stimulation of PAF-synthesis in pulmonary artery endothelial cells by *Staphylococcus aureus* alpha-toxin. *Thromb Res* 1992; 67:243–252
32. Chang SW, Feddersen CO, Henson PM, et al: Platelet-activating factor mediates hemodynamic changes and lung injury in endotoxin-treated rats. *J Clin Invest* 1987; 79:1498–1509
33. Martin C, Goggel R, Ressmeyer AR, et al: Pressor responses to platelet-activating factor and thromboxane are mediated by Rho-kinase. *Am J Physiol Lung Cell Mol Physiol* 2004; 287:L250–L257
34. Salzer WL, McCall CE: Primed stimulation of isolated perfused rabbit lung by endotoxin and platelet activating factor induces enhanced production of thromboxane and lung injury. *J Clin Invest* 1990; 85:1135–1143
35. Rijneveld AW, Weijer S, Florquin S, et al: Improved host defense against pneumococcal pneumonia in platelet-activating factor receptor-deficient mice. *J Infect Dis* 2004; 189:711–716
36. McIntyre TM, Zimmerman GA, Prescott SM: Leukotrienes C4 and D4 stimulate human endothelial cells to synthesize platelet-activating factor and bind neutrophils. *Proc Nat Acad Sci U S A* 1986; 83:2204–2208
37. Uhlig S, Wollin L, Wendel A: Contributions of thromboxane and leukotrienes to PAF-induced impairment of lung function in the rat. *J Appl Physiol* 1994; 77:262–269
38. Harnett KM, Biancani P: Calcium-dependent and calcium-independent contractions in smooth muscles. *Am J Med* 2003; 115(Suppl 3A):24S–30S
39. Gafni J, Munsch JA, Lam TH, et al: Xestospongins: Potent membrane permeable blockers of the inositol 1,4,5-trisphosphate receptor. *Neuron* 1997; 19:723–733
40. Bergner A, Sanderson MJ: ATP stimulates Ca^{2+} oscillations and contraction in airway smooth muscle cells of mouse lung slices. *Am J Physiol Lung Cell Mol Physiol* 2002; 283:L1271–L1279
41. Göggel R, Uhlig S: PAF-induced edema is mediated partly by activation of the inositol trisphosphate (IP_3)-receptor. Abstr. *Am J Respir Crit Care Med* 2000; 161:A418
42. Uehata M, Ishizaki T, Satoh H, et al: Calcium sensitization of smooth muscle mediated by a Rho-associated protein kinase in hypertension. *Nature* 1997; 389:990–994
43. Iliev AI, Djannatian JR, Nau R, et al: Cholesterol-dependent actin remodeling via RhoA and Racl activation by the *Streptococcus pneumoniae* toxin pneumolysin. *Proc Nat Acad Sci U S A* 2007; 104:2897–2902
44. Göggel R, Hoffman S, Nusing R, et al: Platelet-activating factor-induced pulmonary edema is partly mediated by prostaglandin E(2), E-prostanoid 3-receptors, and potassium channels. *Am J Respir Crit Care Med* 2002; 166:657–662
45. Göggel R, Winoto-Morbach S, Vielhaber G, et al: PAF-mediated pulmonary edema: A new role for acid sphingomyelinase and ceramide. *Nat Med* 2004; 10:155–160
46. Nakos G, Tsangaris H, Liokatis S, et al: Ventilator-associated pneumonia and atelectasis: Evaluation through bronchoalveolar lavage fluid analysis. *Intensive Care Med* 2003; 29: 555–563
47. Nakos G, Kitsiouli EI, Tsangaris I, et al: Bronchoalveolar lavage fluid characteristics of early intermediate and late phases of ARDS: Alterations in leukocytes, proteins, PAF and surfactant components. *Intensive Care Med* 1998; 24:296–303
48. Bussolino F, Porcellini MG, Varese L, et al: Intravascular release of platelet activating factor in children with sepsis. *Thromb Res* 1987; 48:619–620
49. Sorensen J, Kald B, Tagesson C, et al: Platelet-activating factor and phospholipase A2 in patients with septic shock and trauma. *Intensive Care Med* 1994; 20:555–561
50. Taylor IK, Ward PS, Taylor GW, et al: Inhaled PAF stimulates leukotriene and thromboxane A2 production in humans. *J Appl Physiol* 1991; 71:1396–1402
51. Bussolino F, Silvagno F, Garbarino G, et al: Human endothelial cells are targets for platelet-activating factor (PAF): Activation of alpha and beta protein kinase C isozymes in endothelial cells stimulated by PAF. *J Biol Chem* 1994; 269:2877–2886
52. Tripathi YB, Lim RW, Fernandez-Gallardo S, et al: Involvement of tyrosine kinase and protein kinase C in platelet-activating-factor-induced c-fos gene expression in A-431 cells. *Biochem J* 1992; 286:527–533
53. Sumita C, Yamane M, Matsuda T, et al: Platelet activating factor induces cytoskeletal reorganization through Rho family pathway in THP-1 macrophages. *FEBS Lett* 2005; 579: 4038–4042

The American Journal of Pathology, Vol. 172, No. 3, March 2008

DOI: 10.2353/ajpath.2008.070834

Endothelial Cysteinyl Leukotriene 2 Receptor Expression Mediates Myocardial Ischemia-Reperfusion Injury

AQ:A-B

Wei Jiang,* Sean R. Hall,* Michael P.W. Moos,* Richard Yang Cao,* Satoshi Ishii,† Kofo O. Ogunyankin,‡ Luis G. Melo,*‡ and Colin D. Funk*§

From the Departments of Physiology, Medicine,‡ and Biochemistry,§ Queen's University, Kingston, Canada; and the Department of Biochemistry and Molecular Biology,† University of Tokyo, Tokyo, Japan*

Cysteinyl leukotrienes (CysLTs) have been implicated as inflammatory mediators of cardiovascular disease. Three distinct CysLT receptor subtypes transduce the actions of CysLTs but the role of the endothelial $CysLT_2$ receptor ($CysLT_2R$) in cardiac function is unknown. Here, we investigated the role of $CysLT_2R$ in myocardial ischemia-reperfusion (I/R) injury using transgenic (tg) mice overexpressing human $CysLT_2R$ in vascular endothelium and nontransgenic (ntg) littermates. Infarction size in tg mice increased 114% compared with ntg mice 48 hours after I/R; this increase was blocked by the CysLT receptor antagonist BAY-u9773. Injection of ^{125}I-albumin into the systemic circulation revealed significantly enhanced extravasation of the label in tg mice, indicating increased leakage of the coronary endothelium, combined with increased incidence of hemorrhage and cardiomyocyte apoptosis. Expression of proinflammatory genes such as Egr-1, VCAM-1, and ICAM was significantly increased in tg mice relative to ntg controls. Echocardiographic assessment 2 weeks after I/R revealed decreased anterior wall thickness in tg mice. Furthermore, the postreperfusion time constant τ of isovolumic relaxation was significantly increased in tg animals, indicating diastolic dysfunction. These results reveal that endothelium-targeted overexpression of $CysLT_2R$ aggravates myocardial I/R injury by increasing endothelial permeability and exacerbating inflammatory gene expression, leading to accelerated left ventricular remodeling, induction of peri-infarct zone cellular apoptosis, and impaired cardiac performance. ***(Am J Pathol 2008, 172:000–000; DOI: 10.2353/ajpath.2008.070834)***

Myocardial infarction results from severe impairment of the coronary blood supply usually provoked by thrombotic or other acute alterations of coronary atherosclerotic plaque.[1] It remains the chief cause of death in North America and Europe.[2] With loss of oxygen supply, apoptosis and necrosis of cardiac myocytes in the ischemic area ensues leading to decreased cardiac performance.[3] Rapid reperfusion is essential to limit the extent of myocardial necrosis. However, the consequences of reperfusion are complex and include various deleterious effects collectively referred to as ischemia-reperfusion (I/R) injury.[1] The intense inflammatory response after reperfusion plays a central role not only in promoting tissue injury, but also in repair after infarction.[4] The inflammatory process characterizing early and late reperfusion is an important aspect of the changes leading to tissue damage.[4] Increased vascular permeability and expression of adhesion molecules initiates the inflammatory reaction, and alterations of endothelial function are pivotal in the development of reperfusion damage.[4,5] Fn1

Cysteinyl leukotrienes (CysLTs), leukotriene C_4 (LTC_4), leukotriene D_4 (LTD_4), and leukotriene E_4 (LTE_4), are well established inflammatory agents that mediate bronchial and vascular smooth muscle constriction and enhance vascular permeability.[6] CysLTs are implicated in inflammatory conditions such as asthma and more recently in cardiovascular disease.[7–9] CysLTs mediate their actions via G protein-coupled receptor (GPCR) proteins, cysteinyl leukotriene 1 receptor ($CysLT_1R$), cysteinyl leukotriene 2 receptor ($CysLT_2R$), and a recently deorphanized GPCR known as GPR17.[8,10] The $CysLT_2R$ gene is ex-

Supported by the Canadian Institutes of Health Research (grants MOP 68930 to C.D.F. and MOP 79506 to L.G.M.), the Heart and Stroke Foundation of Ontario (grant NA 5779 to L.G.M.), and the Pharmacological Society of Canada (Merck Frosst postdoctoral fellowship to S.R.H.).

Accepted for publication November 20, 2007.

This publication is dedicated to the honor of Luis G. Melo who passed away suddenly after a brief and courageous battle with pancreatic cancer.

C.D.F. and L.G.M. hold Canada Research Chairs. C.D.F. is a career investigator of the Heart and Stroke Foundation of Ontario.

Address reprint requests to Colin D. Funk, Department of Physiology, 433 Botterell Hall, Stuart St., Queen's University, Kingston, ON K7L 3N6 Canada. E-mail: funkc@queensu.ca.

balt2/zjh-jpath/zjh-jpath/zjh00308/zjh7551-08z | xppws | S=1 | 1/21/08 | 4:55 | 4/Color Figure(s): F1-4,F6-7 | Art: AJP07-0834 | Input-krb

pressed in human heart and coronary vessels, also within the cardiac Purkinje system, as well as in human coronary smooth muscle cells and umbilical vein endothelial cells.[8,11–14] $CysLT_2R$ expression in mouse heart appears to be more restricted with diffuse expression within endothelial cells.[15] We generated previously transgenic (tg) mice overexpressing the human $CysLT_2R$ in vascular endothelium to characterize the role of this receptor in vascular function.[16]

The involvement of CysLTs and their receptors in inflammation and fibrosis has been confirmed in various animal and human studies.[17] Several studies reported enhanced edema and neutrophil infiltration after myocardial I/R concomitant with elevation of CysLTs.[18,19] These eicosanoids are detected as increased urinary LTE_4 levels in patients after admission for suspected acute myocardial infarction and unstable angina.[20] Moreover, the expression of $CysLT_1R$ and $CysLT_2R$ is increased in organs that are prone to ischemic damage and $CysLT_1R$ antagonism exerts anti-inflammatory effects on cerebral and renal I/R injury.[21–23] Few studies have investigated CysLTs and their receptors in acute myocardial infarction and specifically the role of $CysLT_2R$ in myocardial I/R injury has not been established. Here, we report that endothelium-targeted overexpression of $CysLT_2R$ aggravates myocardial I/R injury by increasing endothelial permeability and exacerbating inflammatory gene expression, leading to accelerated left ventricular (LV) remodeling and impaired cardiac performance.

Materials and Methods

Animals

The generation of EC-$CysLT_2R$ transgenic mice has been described previously.[16] These mice express seven copies of the human $CysLT_2R$ gene under control of the Tie2 promoter/enhancer, integrated in a gene-sparse region of chromosome 6. Hemizygous mice were continuously backcrossed with C57BL/6 mice to obtain equal numbers of transgenic and wild-type littermates. 5-Lipoxygenase-deficient ($5LO^{-/-}$) mice, developed in our laboratory previously,[24] were obtained from The Jackson Laboratory (Bar Harbor, ME). The mice were backcrossed for more than nine generations to the C57BL/6 background. The $5LO^{-/-}$ mice show absence of 5-lipoxygenase mRNA, protein, and leukotriene synthesis in inflammatory cells. $CysLT_2R$-deficient LacZ mice were generated by standard gene targeting procedures using C57BL/6 embryonic stem cells (S. Ishii, unpublished data) and embryos heterozygous for the genetic modification were transferred from Japan, revived at Queen's University, and littermates of heterozygous offspring (all on a C57BL/6 genetic background) were used in these studies.

Mouse Model of Myocardial I/R and Drug Treatment

Mice (8 to 12 weeks) underwent coronary artery occlusion or sham surgery as previously described.[25] Briefly, mice were anesthetized with sodium pentobarbital (45 mg/kg) intraperitoneally, intubated, and ventilated with a rodent ventilator (Harvard Apparatus, St. Laurent, Canada). A midsternal thoracotomy was performed at the fourth intercostal space to expose the anterior surface of the heart. The proximal left anterior descending artery (LAD) was identified and a 6-0 silk Ethilon suture was placed around the artery and surrounding myocardium just below the atrioventricular border. Regional ischemia was induced for 30 minutes by tightening the suture against a small piece of PE-10 tubing placed on top of the LAD. Ischemia was confirmed by the discoloration of the myocardium. Sham-operated animals served as surgical controls and were subjected to the same surgical procedures as the experimental animals, with the exception that the LAD was not ligated. At the end of ischemia, the ligature was loosened and reperfusion was achieved. The lungs were reinflated and the muscle and skin layers were closed separately. The animals were weaned from the ventilator, extubated, and allowed to recover under a heat lamp before being returned to their cages. For animals receiving drug treatment, Bay-u9773 (0.25 mg/kg; Biomol Research Products, Plymouth Meeting, PA) was diluted in 1× phosphate-buffered saline (PBS) and injected intraperitoneally 4 hours before surgery, and 2, 8, and 16 hours after reperfusion. Surgical procedures and treatment regimens were approved by the University Animal Care Committee at Queen's University and adhered to the guidelines of the Canadian Council of Animal Care and the Guiding Principles in the Care and Use of Animals of the American Physiological Society.

Morphometric Evaluation of Risk Area and Infarction Size

Forty-eight hours after reperfusion, mice were euthanized by an intraperitoneal pentobarbital overdose. The 48-hour time point was selected because it is commonly used to assess early inflammatory events (eg, leukocyte infiltration, vascular leakage). The heart was exposed and the original suture was religated. The heart was then perfused retrogradely with 100 to 200 μl of 2% Evans blue dye in PBS (pH 7.4) to delineate the nonischemic area. The heart was excised and rinsed in ice-cold PBS and the LV, including the interventricular septum, was sectioned into four or five slices of similar thickness perpendicular to the long axis of the heart. The slices were incubated in 1% 2,3,5-triphenyltetrazolium chloride (TTC; Sigma Chemicals, St. Louis, MO) at 37°C for 15 minutes to demarcate viable and necrotic tissue. The thickness of each slice was measured using calipers. The slices were photographed on both sides with a digital camera (Canon Corp., Tokyo, Japan). The infarct area (pale white), the area at risk (area excluding Evans Blue), and the total left ventricular area were traced and calculated for both sides of each slice using Image software (National Institutes of Health, Bethesda, MD). The areas for each slice were multiplied by the thickness of the slice to obtain a measure of volume. The cumulative volume for all sections for each heart was used for comparisons. The size

balt2/zjh-jpath/zjh-jpath/zjh00308/zjh7551-08z | xppws | S=1 | 1/21/08 | 4:55 | 4/Color Figure(s): F1–4,F6–7 | Art: AJP07-0834 | Input-krb

of LV at risk was calculated as the ratio of the LV volume excluding Evans blue dye to the total LV volume. Infarct size was calculated as the ratio of the infarct volume to the volume of the risk area as previously described.[26] Animals with infarct volume in the 35 to 70% range of total LV volume were used as inclusion criteria in the study.[27] Only one mouse was excluded based on these criteria.

Lactate Dehydrogenase (LDH) and Creatine Kinase (CK) Activity in Plasma

Biochemical analysis of myocardial injury was performed in heparinized arterial blood collected at termination of the experiment. Plasma LDH and CK were measured using an automated clinical analyzer at the Clinical Analysis at the Kingston General Hospital using clinical grade reagents.

Vascular Permeability Assay in Cardiac Tissue

Forty-eight hours after reperfusion, mice (8 to 12 weeks) were anesthetized by an intraperitoneal injection of pentobarbital (45 mg/kg). ^{125}I-albumin (10^6 cpm/1.44 mCi/mg; MP Biomedicals, Inc., Mississauga, Canada) was injected into the right external jugular vein via a PE-10 catheter. Twenty minutes after injection, the mice were euthanized, and blood was obtained as above and weighed. Exsanguination and removal of excess ^{125}I-albumin proceeded via the right atrium. A 23-gauge needle was inserted into the apex of the left ventricle and the mouse was perfused retrogradely at 40 mmHg with 5.85 ml/100 g of 0.9% NaCl containing 100 U/ml heparin as described previously.[28] The LAD was then religated and Evans blue dye was perfused as above to delineate the risk area, which was then dissected from the remaining myocardial tissue, weighed, and placed in individual tubes. The radioactivity in the blood, nonrisk area, and risk area were counted separately using a gamma counter (Beckman Instruments, Irvine, CA). The permeability index of the different regions was calculated as the radioactivity per g of wet tissue divided by the radioactivity in 1 g of blood.[29] Sham-surgery controls were subjected to the same manipulations, with the exception that the ligature was not tied.

RNA Extraction and Real-Time Polymerase Chain Reaction (PCR)

Total RNA was isolated from the risk area of the left ventricle 3 hours after reperfusion using Trizol reagent (Sigma). Total RNA was reverse-transcribed to cDNA using the Synthesis System for RT-PCR kit (Invitrogen, Carlsbad, CA) according to the manufacturer's protocol. For detection of mouse gene expression, quantitative real-time PCR was performed using a 7500 thermal cycler with TaqMan Universal PCR master mix and TaqMan gene expression assays (Egr-1, VCAM-1, and ICAM-1; Applied Biosystems, Foster City, CA) or with SYBR Green PCR master mix (CysLT$_1$R, and CysLT$_2$R) as described.[16] GAPDH was used as a control housekeeping gene. Data are calculated by the $2^{-}\Delta\Delta$CT method and are presented as fold induction of transcripts for target genes normalized to GAPDH, with respect to the sham controls.[30]

Terminal Deoxynucleotidyl Transferase-Mediated dUTP Nick End-Labeling (TUNEL) Staining

TUNEL assays were performed on LV samples with the CardioTACS *in situ* apoptosis detection kit (Trevigen, Gaithersburg, MD) as described by Takahashi and colleagues[31] with some modification. The hearts were arrested in diastole with 0.2 N KCl 48 hours after reperfusion and perfused with 3.7% neutralized formaldehyde solution. The heart was then excised, postfixed in the same fixative for another 12 hours, then cut into three sections corresponding approximately to the apex, mid-papillary, and base. The slices were embedded in paraffin, cut into 5-μm sections, and transferred to silicon-coated slides. High-power fields (12 to 20 at ×400 magnification) were obtained at the different levels to measure the number of TUNEL-positive cardiomyocyte nuclei in the peri-infarct border and uninfarcted remote zones, respectively. Only nuclei that were clearly located in cardiomyocytes were scored. The number of TUNEL-positive cardiomyocyte nuclei was divided by the total number of nuclei to determine the ratio of TUNEL-positive nuclei.

Immunohistochemical Staining

To determine the numbers of infiltrating leukocytes, formalin-fixed, paraffin-embedded 4-μm sections were mounted on silicon-coated slides and treated with 3% H_2O_2 to block endogenous peroxidase. The sections were incubated for 1 hour at room temperature with rat polyclonal anti-mouse CD45 antibody (PharMingen, San Diego, CA) at a dilution of 1:50. The sections were then incubated with biotinylated rabbit IgG (Vector Laboratories, Burlingame, CA), and CD45 immunoreactivity was visualized using diaminobenzidine substrate. The number of leukocytes in the boundary area was counted in 10 random high-power fields, and the average number in each group was calculated.[32] X-gal staining to determine endogenous CysLT$_2$R expression based on the LacZ reporter gene was performed essentially as described.[33] AQ: C

Echocardiography

Mice (8 to 12 weeks) underwent transthoracic echocardiography 1 day before and 2 weeks after acute I/R using a HP (Phillips) Sonos 5500 equipped with a 15-6L (15-6 MHz) intraoperative linear array transducer essentially as previously described.[34] The 2-week time point was chosen as one of the earliest time points to clearly define remodeling responses in rodents.[34] Briefly, in preparation for echocardiography, animals were lightly anesthe- AQ: D

balt2/zjh-jpath/zjh-jpath/zjh00308/zjh7551-08z | xppws | S=1 | 1/21/08 | 4:55 | 4/Color Figure(s): F1–4,F6–7 | Art: AJP07-0834 | Input-krb

tized by halothane using a nose cone, shaved, and positioned on a heated pad in a recumbent position. Measurements were performed at the midpapillary level from well aligned M-mode images from the parasternal short-axis view. LVd (LV diastolic diameter), PWd (end-diastolic posterior wall thickness), and IVSd (interventricular septum thickness) were determined. The relative wall thickness for each level of the LV was calculated as (PWd + IVSd)/LVd. For each parameter, an average of five cardiac cycles was used for calculations.

Hemodynamic Measurements

Two weeks after acute I/R injury, mice were anesthetized with isoflurane (2%) in medical grade oxygen. The animals were then intubated and ventilated using a pressure controlled respirator (Kent Scientific Corp., Litchfield, CN) at a tidal volume of 200 μl and a frequency of 130 strokes/minute. Body temperature was monitored with a rectal thermometer and maintained at 37°C with the aid of a heat lamp. A midsternal thoracotomy was performed as above to expose the heart. The right jugular vein was cannulated for drug administration. A 1.4F ultra-miniature Millar catheter (SPR 839; Millar Instruments, Houston, TX) was placed into the left ventricle through the apex to record LV pressure. After recording steady-state LV pressures, mice were given an intravenous administration of the synthetic catecholamine dobutamine (10 ng/g body weight) to investigate the functional integrity of adrenergic signaling in the heart. The peak hemodynamic response was recorded using a data acquisition system (PVAN, Millar Instruments). The PVAN software was used for off-line calculation of LV peak systolic pressure, LV end-diastolic pressure, LV peak-positive developed pressure (dP/dt_{max}), LV peak-negative developed pressure (dP/dt_{min}), LV pressure at peak positive developed pressure ($P@dP/dt_{max}$), heart rate, and tau (τ) as described.[35] For calculation of hemodynamic parameters, a minimum of 50 consecutive cardiac cycles were used.

Statistical Analysis

All data are expressed as mean ± SEM. One-way analysis of variance followed by Student-Neuman-Keuls *t*-test were used to compare differences in risk area, infarct size, myocardial enzyme activities, and endothelial permeability, as well as differences in inflammatory gene expression and cardiomyocyte apoptosis. Unpaired *t*-test was used to compare differences in neutrophil infiltration and echocardiographic and functional parameters between tg and ntg mice. Paired *t*-test was used to compare before and after I/R changes in echocardiographic parameters and LV functional responses to dobutamine in the same animals. A P value <0.05 was considered to indicate statistical significance.

Results

CysLT Receptor Expression in Mouse Hearts

The expression of both native murine $CysLT_1R$ and $CysLT_2R$ was examined in hearts by real-time quantitative PCR as previously done in mouse ear tissue.[16] Gene expression for both CysLT receptors was low in noninfarcted ntg hearts and in infarcted hearts 3 hours after I/R injury (Figure 1). However, 48 hours after I/R injury F1
$CysLT_1R$ expression had increased 7.5-fold whereas $CysLT_2R$ expression increased 3.5-fold. The human $CysLT_2R$ transgene, using specific primers that can distinguish between species, could only be detected in tg mice. Using a second independent technique, we were also able to document elevation of $CysLT_2R$ expression after 48 hours of I/R. Thus, using a novel mouse strain in which the *Cysltr2* gene is deleted and replaced with a LacZ reporter gene under control of the *Cysltr2* gene regulatory elements (S. Ishii et al, unpublished data) we were able to demonstrate sparse blue X-gal staining in noninfarcted ventricular tissue and 3 hours after I/R injury (Figure 1, B and C), consistent with the pattern observed previously by *in situ*

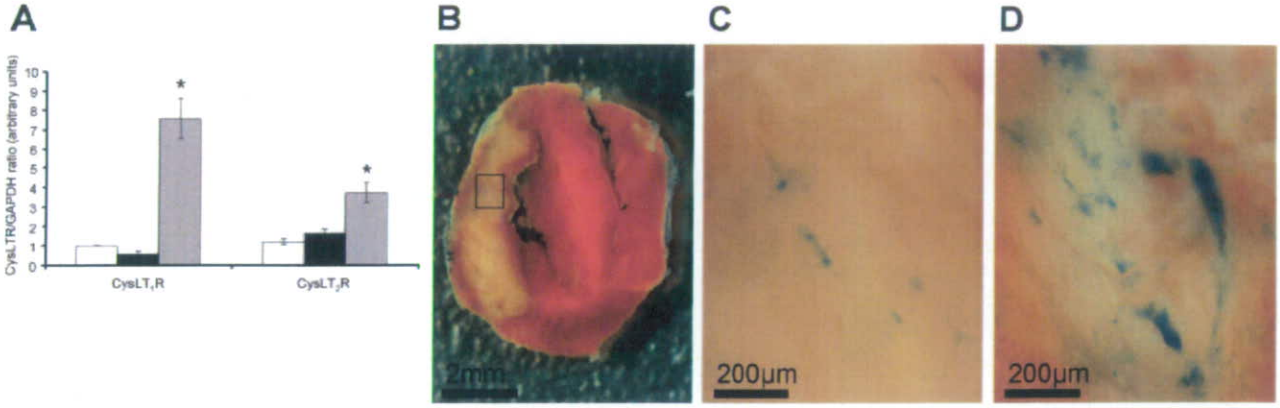

Figure 1. Expression of $CysLT_1R$ and $CysLT_2R$ in mouse hearts. **A:** Quantitative real-time PCR was used to assess gene expression for the two CysLT receptors relative to GAPDH expression in ntg mouse hearts ($n = 3$) as described in the Materials and Methods section. **Open bars**, sham-operated mice; **black bars**, hearts 3 hours after I/R; **cross-hatched bars**, hearts 48 hours after I/R. $^*P < 0.05$ compared to sham-operated controls. **B:** TTC-stained heart slice from a $CysLT_2R$-deficient LacZ mouse 3 hours after I/R injury. **C:** Representative $CysLT_2R$ expression in **boxed region** of the slice shown in **B** detected via the reporter gene LacZ with blue X-gal staining. **D:** $CysLT_2R$ expression (via reporter LacZ/X-gal staining) in a heart slice from a $CysLT_2R$-deficient LacZ mouse having undergone 48 hours of I/R. Similar patterns of expression were observed in two additional mice at 3 and 48 hours after I/R.

balt2/zjh-jpath/zjh-jpath/zjh00308/zjh7551-08z | xppws | S=1 | 1/21/08 | 4:55 | 4/Color Figure(s): F1–4,F6–7 | Art: AJP07-0834 | Input-krb

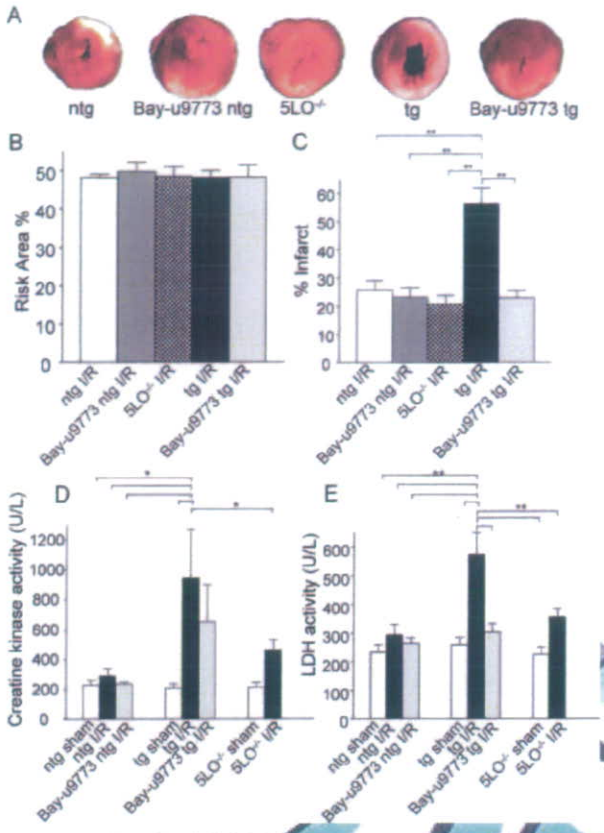

Figure 2. Effect of endothelial $CysLT_2R$ overexpression on LV infarct size after acute I/R injury. **A:** Representative TTC-stained ventricular sections from ntg, tg, and $5LO^{-/-}$ mice at 48 hours after I/R. Representative sections of ntg and tg mice treated with the nonselective dual $CysLT_1R/CysLT_2R$ receptor antagonist Bay-u9773 are also shown. **B:** Morphometric analysis of LV area at risk (**B**) and infarct size (**C**) in the five groups mentioned above. **D** and **E:** Serum levels of CK (**D**) and LDH (**E**) in sham and infarcted ntg, tg, and $5\text{-}LO^{-/-}$ mice at 48 hours after reperfusion. $^*P < 0.05$; $^{**}P < 0.01$; $n = 8$ for groups in **A–C**; $n = 6$ for groups in **D** and **E**.

hybridization in normal mouse heart.[15] After 48 hours of I/R injury, staining intensity increased in the infarct and peri-infarct zones (Figure 1D), which was in harmony with the PCR data.

Endothelial $CysLT_2R$ Overexpression Increases Myocardial Infarct Size after LAD Occlusion and Reperfusion

The effect of endothelial overexpression of $CysLT_2R$ on myocardial I/R injury is shown in Figure 2. Gross histological analysis of TTC-stained sections 48 hours after reperfusion showed a larger necrotic area in tg animals compared to ntg littermates and 5-lipoxygenase-null $5LO^{-/-}$ mice (Figure 2A). Histomorphometric analysis revealed that infarct size in $CysLT_2R$ tg mice was increased by 114% relative to ntg mice (56 ± 15% versus 26 ± 9%, $n = 8$, $P < 0.01$) (Figure 2C), despite comparable risk area in all groups (Figure 1B). Infarct size in the $5LO^{-/-}$ null mice was comparable to ntg mice (21 ± 9% versus 26 ± 9%). Treatment of tg mice with the nonselective dual $CysLT_1R/CysLT_2R$ antagonist Bay-u9773, at a dose tested empirically to evoke $CysLT_2R$ antagonism, markedly reduced infarct size by nearly 60% (56% versus 23%, $n = 8$, $P < 0.05$) to levels comparable to ntg and $5LO^{-/-}$ mice (Figure 2, A and C). The antagonist had no additional effect on infarct size in ntg mice.

We measured serum levels of CK and LDH 48 hours after reperfusion. CK (Figure 2D) and LDH (Figure 2E) activities in infarcted ntg mice were increased by ~26% compared to the baseline levels in sham-operated controls. In contrast, CK and LDH levels were markedly elevated by 357% and 123%, respectively, in tg mice subjected to I/R compared to tg sham controls (Figure 2, D and E). Compared to ntg I/R mice, the levels of CK and LDH were elevated by ~230% and 100%, respectively, in tg mice. In concordance with the histopathological findings, treatment with Bay-u9773 reduced levels of CK and LDH after reperfusion in the tg animals (Figure 2, D and E), while having no significant effect on these markers in ntg mice. I/R increased the levels of CK and LDH in $5LO^{-/-}$ mice but this was significantly smaller than in tg mice (Figure 2, D and E).

Endothelial $CysLT_2R$ Overexpression Increases Permeability in the Infarcted Region of Transgenic Mouse Hearts

Previously we detected enhanced vascular permeability responses to leukotriene challenge and passive cutaneous anaphylaxis in mouse ear vasculature of tg mice.[16] To examine if similar vascular responses occur in the coronary endothelium after myocardial I/R, we assessed the histopathology of the infarct. In addition, we measured extravasation of ^{125}I-BSA in the ischemic and remote areas of the left ventricle at 48 hours after reperfusion. Microscopic examination of the infarct in hematoxylin and eosin (H&E)-stained sections showed minimal accumulation of erythrocytes in the infarcted region of ntg mice (Figure 3A). In contrast, tg mice presented significant accumulation of red cells in the interstitium, resulting in hemorrhage of the infarcted area (Figure 3B). Basal coronary endothelial permeability to ^{125}I-BSA did not differ significantly between ntg and tg mice (Figure 3C). I/R injury led to significant interstitial accumulation of ^{125}I-BSA in both ntg and tg mice. However, the increase in coronary circulation permeability was more pronounced in tg versus ntg mice (202% versus 93%, Figure 3C). No differences in permeability were seen in the nonischemic region of the myocardium.

Endothelial $CysLT_2R$ Overexpression Increases $CD45^+$ Leukocyte Infiltration after I/R in Transgenic Mouse Hearts

We used immunostaining of the pan leukocyte cell surface marker CD45 to determine whether the enhanced permeability of coronary endothelium leads to increased leukocyte infiltration of the infarcted region after I/R injury. Figure 4A shows representative cross-sections from the peri-infarct region in ntg and tg mice. The tg mice showed greater density of CD45-positive cells than ntg mice. Morphometric analysis showed

balt2/zjh-jpath/zjh-jpath/zjh00308/zjh7551-08z | xppws | S=1 | 1/21/08 | 4:55 | 4/Color Figure(s): F1–4,F6–7 | Art: AJP07-0834 | Input-krb

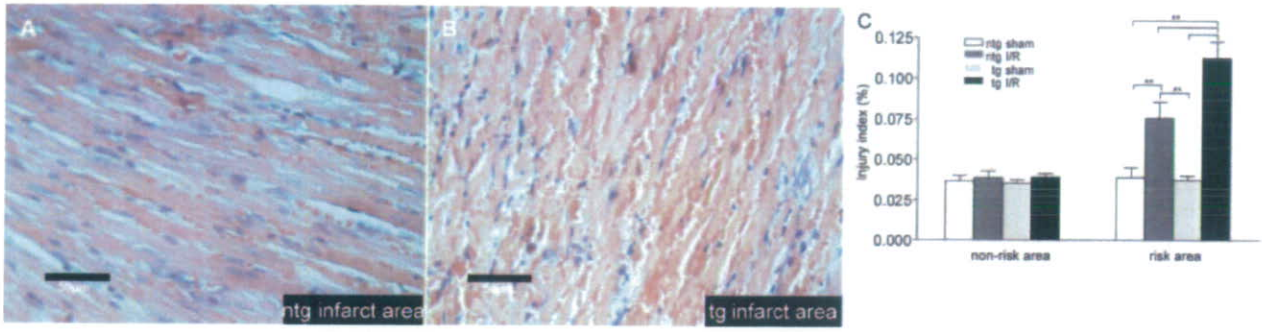

Figure 3. Effect of endothelial $CysLT_2R$ overexpression on myocardial histopathology and coronary endothelial permeability after acute I/R injury. **A** and **B:** Microscopic appearance of infarcted left ventricle in H&E-stained paraffin sections from ntg (**A**) and tg (**B**) mice 48 hours after acute I/R injury. **C:** Permeability of coronary endothelium to ^{125}I-BSA in the at-risk and nonrisk regions of the left ventricle of ntg and tg mice. $^{**}P < 0.01$; $n = 6$. Scale bars = 50 μm.

>100% increase in the number of infiltrating leukocytes in tg compared to ntg mice (1289 ± 113/mm^2 versus 528 ± 131/mm^2) (Figure 4).

Endothelial $CysLT_2R$ Overexpression Increases Egr-1, ICAM, and VCAM-1 Gene Expression in Transgenic Mouse Hearts

To examine potential molecular correlates for the I/R-induced histopathological and permeability alterations seen in tg mice, we determined myocardial mRNA expression of adhesion molecules ICAM and VCAM-1, as well as Egr-1 transcription factor (Figure 5). These genes have been implicated in the myocardial inflammatory response to I/R injury. No significant genotype-related differences were seen in basal expression of these genes. Myocardial expression of ICAM (Figure 5A), VCAM-1 (Figure 5B), and Egr-1 (Figure 5C) were increased significantly in both ntg and tg mice 3 hours after reperfusion. However, the I/R-induced increase in expression of these genes was greater in the tg mice (Figure 5). F5

Endothelial $CysLT_2R$ Overexpression Increases Cardiomyocyte Apoptosis in Transgenic Mouse Hearts

Because apoptosis plays a central role in myocardial cell loss after I/R, we determined whether endothelial overexpression of $CysLT_2R$ influences the number of apoptotic nuclei in cardiomyocytes in the peri-infarct region of tg and ntg mice after I/R. We found increased apoptosis of cells with cardiomyocyte morphology in both groups at 48 hours after reperfusion (Figure 6, A and B). However, the number of apoptotic nuclei in the peri-infarct region of tg animals was significantly greater than in ntg animals (641 ± 222 TUNEL-positive myocytes/10^4 nuclei versus 84 ± 21/10^4 nuclei) (Figure 6B). At 48 hours after reperfusion, cardiomyocyte apoptosis was confined primarily to the peri-infarct region, although at earlier time points (ie, 6 to 24 hours after reperfusion), apoptosis is typically elevated in the infarct core. The number of apoptotic nuclei in the noninfarcted region was markedly lower than in the peri-infarct region and did not differ between ntg and tg mice (Figure 6B). It should be noted that apoptotic nuclei in noncardiomyocytes were observed; however, the precise cell types were not identified nor were they quantified in the present studies. F6

Endothelial $CysLT_2R$ Overexpression Accelerates Left Ventricular Remodeling after I/R

We used two-dimensional echocardiography to examine early (2 week) changes in LV wall and chamber dimensions after I/R. We chose the I/R model of myocardial infarction because it recapitulates some of the features of pathology after infarction seen in humans with reperfused MI, namely slow-developing LV remodeling that is generally complete by 3 to 6 weeks in rodents.[36,37] Repre-

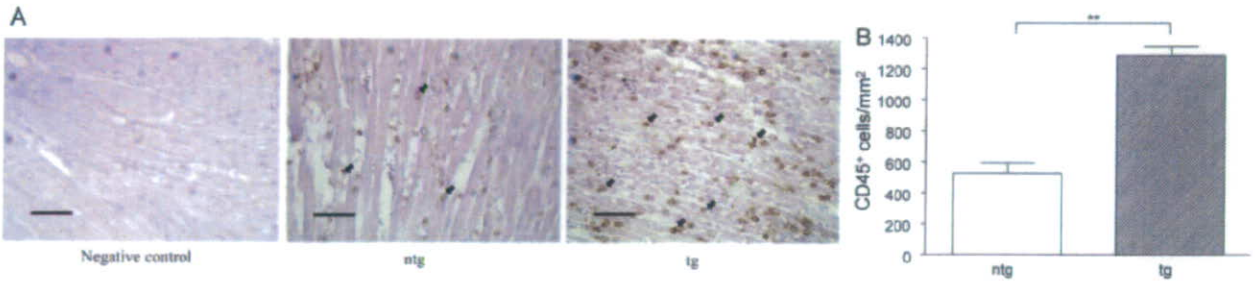

Figure 4. Effect of endothelial $CysLT_2R$ overexpression on leukocyte infiltration after I/R. **A:** Representative photomicrographs showing immunohistochemical detection of pan-leukocyte cell surface marker CD45 in the peri-infarct region of the LV in ntg and tg mice at 48 hours after reperfusion. **Arrows** indicate CD45-positive cells. **B:** Quantitative morphometric analysis of leukocyte infiltration. $^{**}P < 0.01$; $n = 4$. Scale bars = 50 μm. Original magnifications, ×400.

balt2/zjh-jpath/zjh-jpath/zjh00308/zjh7551-08z | xppws | S=1 | 1/21/08 | 4:55 | 4/Color Figure(s): F1–4,F6–7 | Art: AJP07-0834 | Input-krb

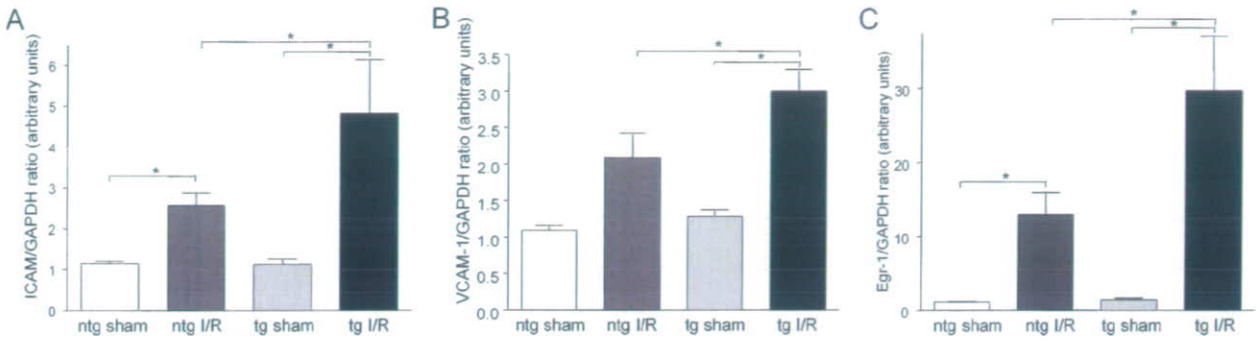

Figure 5. Effect of endothelial CysLT$_2$R overexpression on proinflammatory gene expression. **A–C:** Quantitative real-time PCR evaluation of ICAM (**A**), VCAM-1 (**B**), and Egr-1 (**C**) gene expression in total RNA extracted from the ischemic area of mouse hearts at 3 hours after reperfusion. $^*P < 0.05$; $n = 3$.

sentative M-mode frames taken before and 2 weeks after acute I/R injury are shown in Figure 7, and echocardiographic data are summarized in Table 1. Pre-I/R wall and chamber dimensions did not differ significantly between ntg and tg mice, with the exception of left ventricular diastolic dimension (LVDd) that was found to be slightly increased in tg mice (Figure 7, A and C; Table 1). Two weeks after reperfusion the tg mice presented significant thinning of the anterior wall/interventricular septum whereas the anterior wall remained relatively unchanged in ntg mice (Figure 7, B and D; Table 1). Systolic and diastolic LV chamber dimensions after infarction remained relatively unchanged from preinfarction values in ntg mice (Figure 7, C and D; Table 1). However, tg mice showed a trend toward greater LV systolic dimension after infarction than ntg mice (21% versus 12% increase with respect to preinfarction values; Figure 7, A and B, and Table 1).

Endothelial CysLT$_2$R Overexpression Impairs Left Ventricular Function after I/R

We also assessed the effect of endothelial CysLT$_2$R overexpression on LV function using a microtip pressure catheter (Table 2). Basal LV function did not differ significantly between ntg and tg mice. Furthermore, both types of mice responded comparably to an acute bolus injection of dobutamine with increases in heart rate, LV pressures, and maximal and minimal values of the first derivative of LV pressure (Table 2). Two weeks after I/R, function remained relatively unchanged in ntg mice. In contrast, tg animals showed a trend toward decreased LV +dP/dt and LV −dP/dt and a significant increase in the time constant of isovolumic relaxation (τ), indicating the presence of both systolic and diastolic dysfunction (Table 2). Interestingly, both genotypes showed refractoriness of heart rate and LV pressures to dobutamine after infarction.

Discussion

The endothelium plays a pivotal role in maintaining vessel homeostasis by elaborating a variety of vasoactive, anti-inflammatory and antithrombotic factors that help maintain coronary vessel tone and protect the vessel wall against inflammatory cell and platelet adhesion.[38] Endothelial dysfunction plays a central role in the pathogenesis of myocardial I/R injury[1,5,18] and is characterized by impaired vessel relaxation, and enhanced expression of

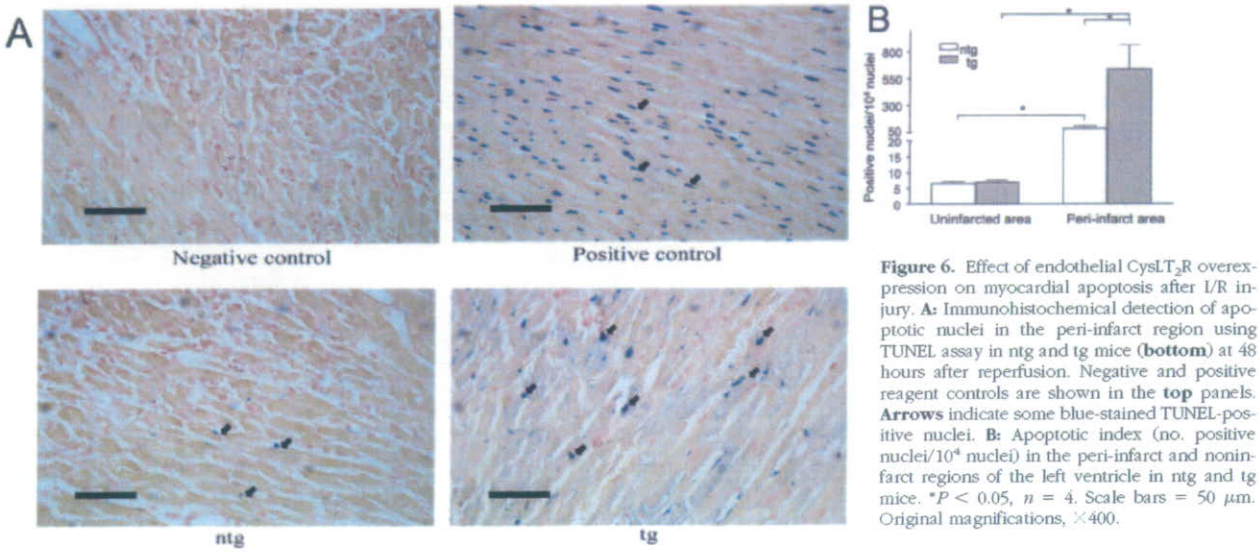

Figure 6. Effect of endothelial CysLT$_2$R overexpression on myocardial apoptosis after I/R injury. **A:** Immunohistochemical detection of apoptotic nuclei in the peri-infarct region using TUNEL assay in ntg and tg mice (**bottom**) at 48 hours after reperfusion. Negative and positive reagent controls are shown in the **top** panels. **Arrows** indicate some blue-stained TUNEL-positive nuclei. **B:** Apoptotic index (no. positive nuclei/10^4 nuclei) in the peri-infarct and noninfarct regions of the left ventricle in ntg and tg mice. $^*P < 0.05$, $n = 4$. Scale bars = 50 μm. Original magnifications, ×400.

balt2/zjh-jpath/zjh-jpath/zjh00308/zjh7551-08z | xppws | S=1 | 1/21/08 | 4:55 | 4/Color Figure(s): F1–4,F6–7 | Art: AJP07-0834 | Input-krb

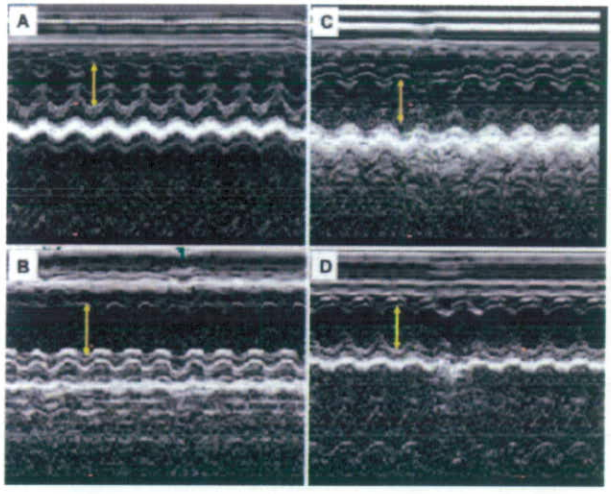

Figure 7. Effect of endothelial $CysLT_2R$ overexpression on left ventricular wall and chamber dimensions. **A–D:** Representative M-mode frames from the mid-papillary region of tg (**A**, **B**) and ntg (**C**, **D**) before (**A**, **C**) and 2 weeks after (**B**, **D**) acute I/R injury. **Arrow** indicates width of the LV chamber.

inflammatory and adhesion molecules, leading to increased vascular permeability, inflammatory cell infiltration, and platelet adhesion and thrombus formation. CysLTs are major inflammatory mediators and activation of endothelial $CysLT_2R$ markedly increases vascular permeability in transgenic mice.[16] We now report that myocardial injury in response to acute I/R is exacerbated in endothelium-targeted $CysLT_2R$ transgenic mice, in association with increased coronary vascular permeability, inflammatory cell infiltration, and heightened myocyte loss through apoptosis.

CysLT synthesis increases in humans[20] with myocardial infarction. Furthermore, pretreatment with leukotriene biosynthesis inhibitors, AA-861 or Bay X1005, reduces neutrophil influx and infarct size after I/R injury in rats[39] and rabbits,[40] respectively, and intravenous infusion of a CysLT receptor antagonist LY-171883 at reperfusion decreases infarct size and improves LV functional recovery after myocardial infarction in cats.[41] In addition, recent linkage analysis studies revealed increased risk of stroke and myocardial infarction in some ethnic groups harboring a distinct haplotype in the *ALOX5AP* gene encoding 5-lipoxygenase-activating protein.[42] Thus, it is plausible in the current study that CysLTs released from resident and/or circulating inflammatory cells or synthesized by transcellular pathways between interacting neutrophils and endothelial cells[40,43] may activate $CysLT_2Rs$ in vascular endothelium to promote endothelial leakage and subsequent myocardial damage. CysLTs influence the adhesion of neutrophils to endothelium by up-regulating adhesion molecules[44,45] and may also act as chemotactic factors in recruitment of leukocytes to the infarcted myocardium. There is compelling evidence that activation of $CysLT_2R$ in cultured human endothelial cells leads to activation of a distinct set of immediate-early gene signatures[46] including the transcription factor Egr-1 and a variety of signaling and adhesion molecules that have been shown to participate in ischemic stress and reperfusion injury in mice.[47] In agreement with these findings, the expression of Egr-1, as well as ICAM and VCAM-1 genes, were elevated in the present study after activation of the human transgene in vascular endothelium, suggesting that they may contribute to the enhanced endothelial permeability and neutrophil infiltration in the infarcted myocardium of tg mice.

To examine the relative impact of transgenic endothelial overexpression of $CysLT_2$ receptor vis-à-vis mice native $CysLT_2$ expression after I/R, a number of tests were performed, including analysis of the expression level of $CysLT_1$ and $CysLT_2$ receptors before and after injury (Figure 1), as well as comparative analysis of treatment with the dual $CysLT_1/CysLT_2$ receptor antagonist Bay-u9773, combined with infarction analysis of 5LO/leukotriene-deficient mice (Figure 2). Real-time PCR analysis indicated low levels of native murine $CysLT_1$ and $CysLT_2$ receptors in sham-operated mouse hearts and early after I/R (3 hours) with significantly higher levels of both receptors 48 hours after I/R. We speculate that the increased $CysLT_1R$ levels at 48 hours of I/R are attributable to infiltrating mononuclear leukocytes, a predominant cell type at this time point[32] and cells known to express this receptor subtype.[48] Based on the blue X-gal/LacZ staining in heart tissue as a surrogate for $CysLT_2R$ expression, enhanced expression of this receptor subtype after 48 hours of I/R in the infarct and peri-infarct zones was observed (Figure 1). Although the specific cell types expressing the induced receptor were not positively identified, several cell types including vascular smooth muscle[12] and endothelial cells,[15] Purkinje conducting cells,[11]

Table 1. Two-Dimensional Echocardiographic Analysis of Left Ventricular Wall and Chamber Dimension before and 2 Weeks after Acute Myocardial I/R in $CysLT_2R$ Transgenic and Nontransgenic Mice

	Pre-ischemia/reperfusion		Post-ischemia/reperfusion		% change from pre I/R	
	ntg	tg	ntg	tg	ntg	tg
LVDd (mm)	0.350 ± 0.010	0.389 ± 0.0120*	0.378 ± 0.0087	0.424 ± 0.0300	8.6 ± 4.4	8.8 ± 6.5
LVDs (mm)	0.200 ± 0.0090	0.229 ± 0.0173	0.220 ± 0.0185	0.27 ± 0.0342	11.5 ± 10.2	20.9 ± 15.9
IVSd (mm)	0.0751 ± 0.0030	0.0707 ± 0.0022	0.0727 ± 0.0025	0.0712 ± 0.0008	−2.6 ± 4.0	1.3 ± 3.8
IVSs (mm)	0.127 ± 0.0047	0.125 ± 0.0083	0.118 ± 0.0085	0.103 ± 0.0067†	−6.1 ± 8.8	−16.9 ± 4.3
PWd (mm)	0.0719 ± 0.0017	0.0763 ± 0.0044	0.0811 ± 0.0045	0.0867 ± 0.0041	13.9 ± 8.4	16.7 ± 11.2
PWs (mm)	0.124 ± 0.0052	0.125 ± 0.0044	0.143 ± 0.0148	0.148 ± 0.0060†	15.9 ± 11.4	19.6 ± 7.6
HR (bpm)	472 ± 17	479 ± 30	476 ± 21	481 ± 40	1.2 ± 4.9	0.30 ± 4.6

LVDd, left ventricular chamber diameter at diastole; LVDs, left ventricular chamber diameter at systole; IVSd, interventricular septum thickness at diastole; IVSs, interventricular septum thickness at systole; PWd, posterior wall thickness at diastole; PWs, posterior wall thickness at systole; HR, heart rate. *$P < 0.05$, tg versus ntg by unpaired *t*-test; †$P < 0.05$, pre-I/R versus post-I/R by paired *t*-test.

balt2/zjh-jpath/zjh-jpath/zjh00308/zjh7551-08z | xppws | S=1 | 1/21/08 | 4:55 | 4/Color Figure(s): F1–4,F6–7 | Art: AJP07-0834 | Input-krb

Table 2. Left Ventricular Function in Control CysLT$_2$R-Transgenic and Nontransgenic Mice and 2 Weeks after Acute Myocardial I/R Injury

	ntg				tg			
	Control (n = 6)		I/R (n = 5)		Control (n = 5)		I/R (n = 5)	
	Before DB	After DB	Before DB	After DB	Before DB	After DB	Before DB	After DB
Heart rate, beats/minute	633 ± 14	709 ± 17*	616 ± 26	664 ± 44	575 ± 13‡	642 ± 11*‡	519 ± 32‡	522 ± 39†‡
LV function								
LV peak pressure, mmHg	71 ± 2	138 ± 13*	69 ± 4	72 ± 3	74 ± 4	130 ± 14*	70 ± 4	83 ± 8
LVESP, mmHg	70 ± 2	138 ± 13*	68 ± 4	71 ± 3	72 ± 4	130 ± 14*	70 ± 4*	83 ± 8†
LVEDP, mmHg	3. ± 0	5 ± 1	3 ± 0.3	4 ± 0.4	5 ± 1	7 ± 1*	4 ± 0.6	4 ± 0.2
LV +dP/dt, mmHg/second	5636 ± 320	16,046 ± 1281*	6409 ± 425	9952 ± 1557*†	6571 ± 604	13,921 ± 1867*	4896 ± 569	7412 ± 1728†
LV −dP/dt, mm Hg/second	−6058 ± 423	−10,377 ± 648*	−6624 ± 489	−6454 ± 397†	−6267 ± 621	−9144 ± 680*	−4865 ± 662	−5370 ± 735†
τ, ms	6.37 ± 0.44	5.10 ± 0.19*	5.91 ± 0.33	4.94 ± 0.17*	5.76 ± 0.22	5.77 ± 0.20‡	7.91 ± 0.82†	7.17 ± 0.77‡

DB, dobutamine; LV, left ventricle; LVESP, left ventricular end-systolic pressure; LVEDP, left ventricular end-diastolic pressure; LV +dP/dt, maximal value of the first derivative of LV pressure; LV −dP/dt, minimal value of the first derivative of LV pressure; τ, time constant for isovolumic relaxation.
*$P < 0.05$ after DB versus before DB; †$P < 0.05$, control versus I/R; ‡$P < 0.05$ tg versus ntg.

mesenchymal stem cells, and perhaps some leukocytes are possible candidates.

Bay-u9773 is a nonspecific antagonist of CysLT$_1$R and CysLT$_2$R, rendering it difficult to determine the precise contributions of each receptor subtype to ischemic injury. This is further complicated by the recent discovery of a third CysLT receptor subtype termed GPR17, that can bind CysLT$_1$R antagonists and was found to participate in focal rat brain ischemic injury.[10] Therefore, depending on the organ and tissue-specific vascular beds, various CysLT receptor subtypes might contribute to inflammatory vascular permeability changes in ischemic injury. In our studies, absence of leukotriene ligand to CysLT$_2$R, as represented in 5LO-deficient mice, and in preliminary studies with the recently acquired CysLT$_2$R-deficient LacZ mice (n = 3, data not shown), lack of ligand/receptor did not significantly influence myocardial injury compared to ntg mice. These data are consistent with those in a recent study showing that I/R injury did not differentially affect infarct size in 5LO-deficient mice compared to wild-type controls[49] but apparently not in agreement with the studies mentioned above with leukotriene biosynthesis inhibitors.[39,40] Moreover, the finding that Bay-u9773 did not reduce infarct size below baseline levels in ntg mice suggests that endogenous CysLT$_2$R does not play a significant role in I/R injury in contrast to the transgenic overexpression of the receptor. However, the observation that I/R induces murine CysLT$_2$R in our study at 48 hours, along with a recent report examining CysLT$_2$R expression in human brain tissue finding increased expression in microvascular endothelium after traumatic injury,[50] warrants further study to examine the pathophysiological sequelae of induction of CysLT$_2$R.

The mechanism by which endothelial CysLT$_2$R overexpression leads to increased myocyte apoptosis is not known. To our knowledge no direct role of CysLT$_2$R in cardiomyocyte apoptosis has been established. The cascade of events leading to myocyte apoptosis during I/R involves the activation of both the intrinsic mitochondrial proapoptotic pathway as well as the extrinsic pathway mediated by cytokine activation of death receptors.[51] Myocytes are particularly prone to apoptosis during reperfusion,[52] where up to 30% in the risk area may undergo apoptosis in the first few hours after reperfusion. The events of reperfusion that lead to cardiomyocyte apoptosis have not been fully elucidated. However, reactive oxygen species and cytokines produced by infiltrating inflammatory cells appear to play a central role in activating apoptotic pathways in myocytes.[52,53] For example, genetic mouse models harboring deletions of tumor necrosis factor-α and CD18 genes show reduced infarct size in response to I/R in association with decreased neutrophil infiltration, whereas null mice for the anti-oxidant gene heme oxygenase-1 have increased infarct size and reduced LV recovery in parallel with a decrease in antioxidant load.[52] In the current study, the enhanced influx of CD45$^+$ leukocytes, presumably mostly neutrophils, after reperfusion in CysLT$_2$R tg mice could potentially contribute to the enhanced myocyte apoptosis seen in these animals by a similar mechanism; however, additional mechanisms may also be at play. Regardless of mechanism, the increased apoptosis in tg mice would predictably lead to greater long-term loss of myocardial contractile mass, resulting in LV chamber remodeling and impairment of contractile function. Indeed, in the current study, CysLT$_2$R mice show accelerated LV remodeling, highlighted by decreased anterior wall thickness and increased LV systolic dimensions 2 weeks after reperfusion. Typically, LV remodeling in mice with reperfused myocardium is slow and often absent,[37]

balt2/zjh-jpath/zjh-jpath/zjh00308/zjh7551-08z | xppws | S=1 | 1/21/08 | 4:55 | 4/Color Figure(s): F1–4,F6–7 | Art: AJP07-0834 | Input-krb

AQ: E

unless a significant amount of the LV (>40% of the AAR) is infarcted. Our results indicate that tg $CysLT_2R$ mice had significantly larger infarcts than the ntg counterparts. We presume that the heightened apoptosis is, at least partially, responsible for the larger infarct sizes and subsequent LV remodeling in these mice.

As expected, LV remodeling in tg mice was accompanied by impaired LV function after reperfusion. We believe that this is directly attributable to the greater myocyte loss in tg mice, because basal LV function and responsiveness to β-adrenergic stimulation did not differ significantly between the two groups of animals. In contrast, ntg mice were able to preserve LV function after reperfusion because of the significantly smaller infarcts and absence of negative remodeling. Interestingly, both genotypes showed marked refractoriness to dobutamine after reperfusion. The mechanism underlying this lack of response appears to be unrelated to $CysLT_2R$ overexpression, because it is also present in ntg controls. β-Adrenergic receptor desensitization usually occurs after myocardial infarction as the sympathetic nervous system attempts to maintain hemodynamic homeostasis. However, desensitization usually occurs throughout a longer time course than in the current studies, and is unlikely to be the explanation for the postreperfusion refractoriness to dobutamine.

In summary, the results of the current study indicate that endothelial-targeted overexpression of $CysLT_2R$ exacerbates myocardial injury after ischemia/reperfusion in association with increased inflammatory cell infiltration and cardiomyocyte apoptosis. Inhibition of endothelial $CysLT_2R$ activity should be explored further as a potential strategy for myocardial protection.

Acknowledgments

We thank Caroline Machado and the staff at the Queen's University Transgenic Animal Facility for performing the embryo transfer procedures to obtain $CysLT_2R$-deficient LacZ mice.

References

1. Buja LM: Myocardial ischemia and reperfusion injury. Cardiovasc Pathol 2005, 14:170–175
2. Moens AL, Claeys MJ, Timmermans JP, Vrints CJ: Myocardial ischemia/reperfusion-injury, a clinical view on a complex pathophysiological process. Int J Cardiol 2005, 100:179–190
3. Park JL, Lucchesi BR: Mechanisms of myocardial reperfusion injury. Ann Thorac Surg 1999, 68:1905–1912
4. Di Napoli P, Taccardi AA, De Caterina R, Barsotti A: Pathophysiology of ischemia-reperfusion injury: experimental data. Ital Heart J 2002, 3(Suppl 4):24S–28S
5. Lefer AM, Tsao PS, Lefer DJ, Ma XL: Role of endothelial dysfunction in the pathogenesis of reperfusion injury after myocardial ischemia. FASEB J 1991, 5:2029–2034
6. Funk CD: Prostaglandins and leukotrienes: advances in eicosanoid biology. Science 2001, 294:1871–1875
7. Funk CD: Leukotriene modifiers as potential therapeutics for cardiovascular disease. Nat Rev Drug Disc 2005, 4:664–672
8. Hui Y, Funk CD: Cysteinyl leukotriene receptors. Biochem Pharmacol 2002, 64:1549–1557
9. Folco G, Rossoni G, Buccellati C, Berti F, Maclouf J, Sala A: Leukotrienes in cardiovascular diseases. Am J Respir Crit Care Med 2000, 161:S112–S116
10. Ciana P, Fumagalli M, Trincavelli ML, Verderio C, Rosa P, Lecca D, Ferrario S, Parravicini C, Capra V, Gelosa P, Guerrini U, Belcredito S, Cimino M, Sironi L, Tremoli E, Rovati GE, Martini C, Abbracchio MP: The orphan receptor GPR17 identified as a new dual uracil nucleotides/cysteinyl-leukotrienes receptor. EMBO J 2006, 25:4615–4627
11. Heise CE, O'Dowd BF, Figueroa DJ, Sawyer N, Nguyen T, Im DS, Stocco R, Bellefeuille JN, Abramovitz M, Cheng R, Williams DL Jr, Zeng Z, Liu Q, Ma L, Clements MK, Coulombe N, Liu Y, Austin CP, George SR, O'Neill GP, Metters KM, Lynch KR, Evans JF: Characterization of the human cysteinyl leukotriene 2 receptor. J Biol Chem 2000, 275:30531–30536
12. Takasaki J, Kamohara M, Matsumoto M, Saito T, Sugimoto T, Ohishi T, Ishii H, Ota T, Nishikawa T, Kawai Y, Masuho Y, Isogai T, Suzuki Y, Sugano S, Furuichi K: The molecular characterization and tissue distribution of the human cysteinyl leukotriene CysLT(2) receptor. Biochem Biophys Res Commun 2000, 274:316–322
13. Lötzer K, Spanbroek R, Hildner M, Urbach A, Heller R, Bretschneider E, Galczenski H, Evans JF, Habenicht AJ: Differential leukotriene receptor expression and calcium responses in endothelial cells and macrophages indicate 5-lipoxygenase-dependent circuits of inflammation and atherogenesis. Arterioscler Thromb Vasc Biol 2003, 23:e32–e36
14. Kamohara M, Takasaki J, Matsumoto M, Matsumoto Si, Saito T, Soga T, Matsushime H, Furuichi K: Functional characterization of cysteinyl leukotriene CysLT(2) receptor on human coronary artery smooth muscle cells. Biochem Biophys Res Commun 2001, 287:1088–1092
15. Hui Y, Yang S, Galczenski H, Figueroa DJ, Austin CP, Copeland NG, Gilbert DJ, Jenkins NA, Funk CD: The murine cysteinyl leukotriene 2 (CysLT2) receptor. cDNA and genomic cloning, alternative splicing, and in vivo characterization. J Biol Chem 2001, 276:47489–47495
16. Hui Y, Cheng Y, Smalley I, Jiang W, Goldhahn L, Fitzgerald GA, Funk CD: Directed vascular expression of human cysteinyl leukotriene 2 receptor modulates endothelial permeability and systemic blood pressure. Circulation 2004, 110:3360–3366
17. Kanaoka Y, Boyce JA: Cysteinyl leukotrienes and their receptors: cellular distribution and function in immune and inflammatory responses. J Immunol 2004, 173:1503–1510
18. Frangogiannis NG, Smith CW, Entman ML: The inflammatory response in myocardial infarction. Cardiovasc Res 2002, 53:31–47
19. Barst S, Mullane K: The release of a leukotriene D4-like substance following myocardial infarction in rabbits. Eur J Pharmacol 1985, 114:383–387
20. Carry M, Korley V, Willerson JT, Weigelt L, Ford-Hutchinson AW, Tagari P: Increased urinary leukotriene excretion in patients with cardiac ischemia. In vivo evidence for 5-lipoxygenase activation. Circulation 1992, 85:230–236
21. Yu GL, Wei EQ, Zhang SH, Xu HM, Chu LS, Zhang WP, Zhang Q, Chen Z, Mei RH, Zhao MH: Montelukast, a cysteinyl leukotriene receptor-1 antagonist, dose- and time-dependently protects against focal cerebral ischemia in mice. Pharmacology 2005, 73:31–40
22. Fang SH, Zhou Y, Chu LS, Zhang WP, Wang ML, Yu GL, Peng F, Wei EQ: Spatio-temporal expression of cysteinyl leukotriene receptor-2 mRNA in rat brain after focal cerebral ischemia. Neurosci Lett 2007, 412:78–83
23. Sener G, Sehirli O, Velioglu-Ogunc A, Cetinel S, Gedik N, Caner M, Sakarcan A, Yegen BC: Montelukast protects against renal ischemia/reperfusion injury in rats. Pharmacol Res 2006, 54:65–71
24. Chen XS, Sheller JR, Johnson EN, Funk CD: Role of leukotrienes revealed by targeted disruption of the 5-lipoxygenase gene. Nature 1994, 372:179–182
25. Tarnavski O, McMullen JR, Schinke M, Nie Q, Kong S, Izumo S: Mouse cardiac surgery: comprehensive techniques for the generation of mouse models of human diseases and their application for genomic studies. Physiol Genom 2004, 16:349–360
26. Liu X, Wei J, Peng DH, Layne MD, Yet SF: Absence of heme oxygenase-1 exacerbates myocardial ischemia/reperfusion injury in diabetic mice. Diabetes 2005, 54:778–784
27. Petzelbauer P, Zacharowski PA, Miyazaki Y, Friedl P, Wickenhauser G, Castellino FJ, Groger M, Wolff K, Zacharowski K: The fibrin-derived peptide Bbeta15-42 protects the myocardium against ischemia-reperfusion injury. Nat Med 2005, 11:298–304
28. Schumacher J, Binkowski K, Dendorfer A, Klotz KF: Organ-specific

extravasation of albumin-bound Evans blue during nonresuscitated hemorrhagic shock in rats. Shock 2003, 20:565–568
29. Younger JG, Sasaki N, Delgado J, Ko AC, Nghiem TX, Waite MD, Till GO, Ward PA: Systemic and lung physiological changes in rats after intravascular activation of complement. J Appl Physiol 2001, 90:2289–2295
30. Harja E, Bucciarelli LG, Lu Y, Stern DM, Zou YS, Schmidt AM, Yan SF: Early growth response-1 promotes atherogenesis: mice deficient in early growth response-1 and apolipoprotein E display decreased atherosclerosis and vascular inflammation. Circ Res 2004, 94:333–339
31. Takahashi T, Tang T, Lai NC, Roth DM, Rebolledo B, Saito M, Lew WY, Clopton P, Hammond HK: Increased cardiac adenylyl cyclase expression is associated with increased survival after myocardial infarction. Circulation 2006, 114:388–396
32. Dewald O, Ren G, Duerr GD, Zoerlein M, Klemm C, Gersch C, Tincey S, Michael LH, Entman ML, Frangogiannis NG: Of mice and dogs: species-specific differences in the inflammatory response following myocardial infarction. Am J Pathol 2004, 164:665–677
33. Okada Y, Scott G, Ray MK, Mishina Y, Zhang Y: Histone demethylase JHDM2A is critical for Tnp1 and Prm1 transcription and spermatogenesis. Nature 2007, 450:119–123
34. Liu X, Simpson JA, Brunt KR, Ward CA, Hall SR, Kinobe RT, Barrette V, Tse MY, Pang SC, Pachori AS, Dzau VJ, Ogunyankin K, Melo LG: Pre-emptive heme oxygenase-1 gene delivery reveals reduced mortality and preservation of left ventricular function one year after acute myocardial infarction. Am J Physiol 2007, 293:H48–H59
35. Hall SR, Wang L, Milne B, Hong M: Left ventricular dysfunction after acute intracranial hypertension is associated with increased hydroxyl free radical production, cardiac ryanodine hyperphosphorylation, and troponin I degradation. J Heart Lung Transplant 2005, 24:1639–1649
36. Anversa P, Beghi C, Kikkawa Y, Olivetti G: Myocardial infarction in rats. Infarct size, myocyte hypertrophy and capillary growth. Circ Res 1986, 58:26–37
37. De Celle T, Cleutjens JP, Blankesteijn WM, Debets JJ, Smits JF, Janssen BJ: Long-term structural and functional consequences of cardiac ischemia-reperfusion injury in vivo in mice. Exp Physiol 2004, 89:605–615
38. Rubanyi GM: The role of endothelium in cardiovascular homeostasis and disease. J Cardiovasc Pharmacol 1993, 22:S1–S4
39. Sasaki K, Ueno A, Kswamura M, Katori M, Shigehiro S, Kikawada R: Reduction of myocardial infarct size in rats by selective 5-lipooxygenase inhibitor (AA-861). Adv Prostglandin Thromboxane Leukot Res 1987, 17A:381–383
40. Rossoni G, Sala A, Berti F, Testa T, Buccellati C, Molta C, Muller-Peddinghaus R, Maclouf J, Folco GC: Myocardial protection by the leukotriene synthesis inhibitor BAY X1005: importance of transcellular biosynthesis of cysteinyl-leukotrienes. J Pharmacol Exp Ther 1996, 276:335–341
41. Hock CE, Beck LD, Papa LA: Peptide leukotriene antagonism in myocardial ischemia and reperfusion. Cardiovasc Res 1992, 26:1206–1211
42. Helgadottir A, Manolescu A, Thorleifsson G, Gretarsdottir S, Jonsdottir H, Thorsteinsdottir U, Samani NJ, Gudmundsson G, Grant SF, Thorgeirsson G, Sveinbjornsdottir S, Valdimarsson EM, Matthiasson SE, Johannsson H, Gudmundsdottir O, Gurney ME, Sainz J, Thorhallsdottir M, Andresdottir M, Frigge ML, Topol EJ, Kong A, Gudnason V, Hakonarson H, Gulcher JR, Stefansson K: The gene encoding 5-lipoxygenase activating protein confers risk of myocardial infarction and stroke. Nat Genet 2004, 36:233–239
43. Sala A, Folco G: Neutrophils, endothelial cells, and cysteinyl leukotrienes: a new approach to neutrophil-dependent inflammation? Biochem Biophys Res Commun 2001, 283:1003–1006
44. Pedersen KE, Bochner BS, Undem BJ: Cysteinyl leukotrienes induce P-selectin expression in human endothelial cells via a non-CysLT1 receptor-mediated mechanism. J Pharmacol Exp Ther 1997, 281:655–662
45. Di Gennaro A, Carnini C, Buccellati C, Ballerio R, Zarini S, Fumagalli F, Viappiani S, Librizzi L, Hernandez A, Murphy RC, Constantin G, De Curtis M, Folco G, Sala A: Cysteinyl-leukotrienes receptor activation in brain inflammatory reactions and cerebral edema formation: a role for transcellular biosynthesis of cysteinyl-leukotrienes. FASEB J 2004, 18:842–844
46. Uzonyi B, Lotzer K, Jahn S, Kramer C, Hildner M, Bretschneider E, Radke D, Beer M, Vollandt R, Evans JF, Funk CD, Habenicht AJ: Cysteinyl leukotriene 2 receptor and protease-activated receptor 1 activate strongly correlated early genes in human endothelial cells. Proc Natl Acad Sci USA 2006, 103:6326–6331
47. Yan SF, Fujita T, Lu J, Okada K, Shan Zou Y, Mackman N, Pinsky DJ, Stern DM: Egr-1, a master switch coordinating upregulation of divergent gene families underlying ischemic stress. (Erratum in: Nat Med 2001, 7:500). Nat Med 2000, 6:1355–1361
48. Figueroa DJ, Breyer RM, Defoe SK, Kargman S, Daugherty BL, Waldburger K, Liu Q, Clements M, Zeng Z, O'Neill GP, Jones TR, Lynch KR, Austin CP, Evans JF: Expression of the cysteinyl leukotriene 1 receptor in normal human lung and peripheral blood leukocytes. Am J Respir Crit Care Med 2001, 163:226–233
49. Adamek A, Jung S, Dienesch C, Laser M, Ertl G, Bauersachs J, Frantz S: Role of 5-lipoxygenase in myocardial ischemia-reperfusion injury in mice. Eur J Pharmacol 2007, 57:51–54
50. Hu H, Chen G, Zhang JM, Zhang WP, Zhang L, Ge QF, Yao HT, Ding W, Chen Z, Wei EQ: Distribution of cysteinyl leukotriene receptor 2 in human traumatic brain injury and brain tumors. Acta Pharmacol Sin 2005, 26:685–690
51. Crow MT, Mani K, Nam Y-J, Kitsis RN: The mitochondrial death pathway and cardiac myocyte apoptosis. Circ Res 2004, 95:957–970
52. Eefting F, Rensing B, Wigman J, Pannekoek WJ, Liu WM, Cramer MJ, Lips DJ, Doevendans PA: Role of apoptosis in reperfusion injury. Cardiovasc Res 2004, 61:414–426
53. Duilio C, Ambrosio G, Kuppusamy P, DiPaula A, Becker LC, Zweier JL: Neutrophils are primary source of O2 radicals during reperfusion after prolonged myocardial ischemia. Am J Physiol 2001, 280:H2649–H2657

Immunomodulation by n-3- versus n-6-rich lipid emulsions in murine acute lung injury—Role of platelet-activating factor receptor

Martina Barbara Schaefer, MD; Juliane Ott, DVM; Andrea Mohr; Ming Hua Bi, MD, PhD; Andrea Grosz; Norbert Weissmann, PhD; Satoshi Ishii, PhD; Friedrich Grimminger, MD, PhD; Werner Seeger, MD; Konstantin Mayer, MD

Objective: **Cytokines, platelet-activating factor (PAF), and eicosanoids control local and systemic inflammation. Conventional soybean oil-based lipid emulsions used for parenteral nutrition may aggravate the leukocyte inflammatory response or adhesion to the vessel wall. Fish oil-based lipid emulsions, in contrast, may exert an anti-inflammatory effect.**

Design: **We investigated the impact of lipid emulsions on leukocyte invasion, protein leakage, and cytokines in two murine models of acute inflammation.**

Setting: **Research laboratory of a university hospital.**

Subjects: **Wild-type mice and PAF-receptor knockout mice.**

Interventions: **Mice received an infusion of normal saline, fish oil- or soybean oil-based lipid emulsions before lipopolysaccharide challenge.**

Measurements and Main Results: **Preinfusion with soybean oil resulted in increased leukocyte invasion, myeloperoxidase activity, and protein leakage and exaggerated release of tumor necrosis factor (TNF)-α as well as macrophage inflammatory protein (MIP)-2 into the alveolar space after intratracheal lipopolysaccharide challenge. In contrast, preinfusion with fish oil reduced leukocyte invasion, myeloperoxidase activity, protein leakage, and TNF-α as well as MIP-2 generation. Corresponding profiles were found in plasma following intraperitoneal lipopolysaccharide application: Soybean oil increased but fish oil decreased the TNF-α and MIP-2 formation. When PAF-receptor-deficient mice were challenged with lipopolysaccharide, leukocyte invasion, lung tissue myeloperoxidase, cytokine generation, and alveolar protein leakage corresponded to those observed in wild-type animals. Fish oil and soybean oil lost their diverging effects on leukocyte transmigration, myeloperoxidase activity, leakage response, and cytokine generation in these knockout mice. Similarly, the differential impact of both lipid emulsions on these lipopolysaccharide-provoked changes was suppressed after pretreating animals with a PAF-receptor antagonist.**

Conclusions: **Fish oil- vs. soybean oil-based lipid infusions exert anti- vs. proinflammatory effects in murine models of acute inflammation. The PAF/PAF-receptor-linked signaling appears to be a prerequisite for this differential profile. (Crit Care Med 2007; 35:544–554)**

Key Words: platelet-activating factor; fish oil; lipid emulsions; inflammation; sepsis; acute lung injury

Acute lung injury, the systemic inflammatory response syndrome, and sepsis are common in intensive care patients (1, 2). At early time points, all three entities are associated with an excessive inflammatory response (3), but in later stages of systemic inflammatory response syndrome or sepsis, a reduced immune response may be detected, termed compensatory anti-inflammatory response syndrome (4). Lipids, lipid mediators, and inflammation are closely interrelated (3, 5). The generation of pro- and anti-inflammatory as well as vasoactive eicosanoids (such as prostaglandin E_2, prostaglandin I_2, and thromboxane A_2) is coupled to the generation of free arachidonic acid from phospholipids. In the context of lipids and inflammation, eicosanoids represent a major focus of interest due to their strong proinflammatory and anti-inflammatory potencies (3). Among the n-6 fatty acids in the Western diet and current nutritional regimes applied in intensive care units, linoleic acid is the most prominent fatty acid, giving rise to its elongation and desaturation product and eicosanoid precursor arachidonic acid. The n-3 fatty acids, including eicosapentaenoic acid and docosahexaenoic acid, make up an appreciable part of the fat in cold-water fish and seal meat. Eicosapentaenoic acid-derived 5-series leukotrienes generated by the 5-lipoxygenase and the cyclooxygenase product thromboxane A_3 possess markedly reduced inflammatory and vasomotor potencies compared with the arachidonic acid-derived lipid mediators and may even exert antagonistic functions (6).

In addition to acting as a precursor for eicosanoid formation, n-3 vis-à-vis n-6 fatty acid incorporation into membrane

From the University of Giessen Lung Center (UGLC), Justus-Liebig-University of Giessen, Giessen, Germany (MBS, JO, AM, MHB, AG, NW, FG, WS, KM); and the Department of Biochemistry and Molecular Biology, Faculty of Medicine, The University of Tokyo, Tokyo, Japan (SI).

Supported, in part, by Deutsche Forschungsgemeinschaft, Collaborative Research Center 547 "Kardiopulmonales Gefäßsystem," Project B4 (KM); a postdoctoral grant from the Medical Faculty of the Justus-Liebig University, Giessen (MBS); and a postgraduate scholarship from Altana, Konstanz, Germany (MBS).

Drs. Schaefer and Ott contributed equally to the work and share first authorship. This article includes portions of the doctoral thesis of Juliane Ott.

Dr. Mayer has received speaking fees from B Braun, Baxter, and Fresenius Kabi. The remaining authors have not disclosed any potential conflicts of interest.

DOI: 10.1097/01.CCM.0000253811.74112.B6

(phospho)-lipid pools was suggested to influence lipid-related intracellular signaling events (7). Subclasses of phosphatidylcholine such as the platelet-activating factor (PAF)-precursor pool, as well as phosphatidylinositol and sphingomyelin pools, may be particularly relevant in this respect. Next, gene transcription is modulated as nuclear translocation of nuclear factor-κB and is inhibited by n-3 fatty acids involving signaling by plasma membrane translocation and activation of protein kinase C (8). Furthermore, research work has linked a specific genetic background to the reduction in proinflammatory cytokine generation in volunteers (9).

PAF is a major lipid mediator derived in two steps from phosphatidylcholine yielding free arachidonic acid and the active mediator (10). Furthermore, PAF-like molecules may be generated by oxidative attack on unsaturated fatty acids in phosphatidylcholine, which may aggravate sepsis and tissue injury (11). PAF promotes adhesion of leukocytes to endothelial cells, and application of PAF-receptor antagonists (PAF-RA) ameliorates features of sepsis and shock in experimental models (12), but effects on mortality in septic patients were not reported in clinical phase III studies (13, 14). Mice carrying a targeted disruption of the PAF-receptor (PAF-R) gene exhibit an ameliorated response to an acid-aspiration lung injury model; however, they remain sensitive to lipopolysaccharide (LPS) and endotoxin-induced shock (15).

Different groups reported a major influence of nutrition including n-3 fatty acids on morbidity of intensive care patients. In the adult respiratory distress syndrome, a tailored nutrition with eicosapentaenoic acid, γ-linoleic acid, and antioxidants was reported to improve oxygenation, reduce length of mechanical ventilation, decrease incidence of new organ failures, and shorten length of stay in the intensive care unit (16). Using fish oil supplements, however, several days to weeks are required to effectively influence the fatty acid composition of membrane (phospho)-lipids and thereby the lipid mediator profile in humans (17). In contrast, when administering a fish oil-based lipid emulsion via the intravenous route in volunteers or septic patients, we recently demonstrated rapid changes in cell membrane fatty acid composition and leukocyte functions (18, 19).

In the present study, we developed a murine model suitable for continuous long-term intravenous lipid infusions and subsequently submitted mice to intratracheal or intraperitoneal LPS injection. In addition to analyzing systemic cytokine generation, we focused on compartmentalized inflammatory events such as cytokine appearance in the bronchoalveolar space and recruitment of leukocytes to the alveolar compartment.

MATERIALS AND METHODS

Reagents. Lipoven 10% (soybean oil, or SO) and Omegaven 10% (fish oil, or FO) were purchased from Fresenius-Kabi (Bad Homburg, Germany). Analysis of fatty acid composition of the lipid emulsions is given in Table 1. Chemicals of highest purity were obtained from Merck (Darmstadt, Germany). LPS (O111:B4) from *Escherichia coli* was from Sigma-Aldrich (Dreisenhofen, Germany). The PAF antagonist BN52021 originated from Biomol (Hamburg, Germany).

Animals. Local government authorities and university officials responsible for animal protection approved the study. Parent and offspring PAF-R −/− mice on the BALB/c background and wild-type animals (WT) were kept under standard conditions with a 12-hr day/night cycle under specific pathogen-free conditions. Animals 8–12 wks old (18–21 g weight) were used for experiments. For implantation of a jugular vein catheter, mice were anesthetized by an intraperitoneal injection of a 1:1 mixture of xylazine at 80–100 mg per kilogram of body weight (Bayer, Leverkusen, Germany)/ketamine (Pharmacia & Upjohn, Erlangen, Germany). When animals were anesthetized and spontaneously breathing, points of incisions were shaved and disinfected. A silicon catheter (Braun, Melsungen, Germany) was inserted into the left jugular vein and tied.

Table 1. Fatty acid composition of the soybean oil (SO)-based and fish oil (FO)-based lipid-emulsion (g/L)

Fatty Acid	SO	FO
C14:0	—	4.9
C16:0	12.4	10.7
C16:1n-7	—	8.2
C18:0	5.0	2.4
C18:1n-9	24.1	12.3
C18:2n-6	52.2	3.7
C18:3n-3	8.2	1.3
C20:4n-6	—	2.6
C20:5n-3	—	18.8
C22:5n-3	—	2.8
C22:6n-3	—	16.5
Others	—	16.1

The SO-based emulsion (Lipoven) and the FO-based lipid emulsion (Omegaven) were manufactured with identical techniques and additives. Repetitive gas chromatographic controls of both lipid emulsions revealed <0.3% free eicosapentaenoic acid or arachidonic acid as related to the esterified amounts of these fatty acids.

The catheter was tunneled to the neck of the animal and connected to an osmotic minipump (Alzet, Cupertino, CA) filled with NaCl 0.9% situated in an external device tied to the back allowing easy access and exchange of pumps without anesthesia.

Murine Model of Acute Lung Injury. Mice were anesthetized with xylazine/ketamine, a small catheter was inserted in the trachea, and LPS (0, 1, or 10 μg in 50 μL of normal saline/mouse) was instilled. Twenty-four hours after LPS application, mice were killed by an overdose of isoflurane (Abbot, Wiesbaden, Germany), and bronchoalveolar lavage (BAL) was performed as described (20). An additional BAL was performed after 4 hrs in mice receiving 10 μg of LPS as a precaution since the escalation in LPS dose could have increased mortality in the model. However, even after receiving the higher dose of LPS, all animals survived the observation period. Alveolar-recruited leukocytes recovered from lungs of LPS-challenged and control mice were counted in a counting chamber. Differentiation of leukocytes in blinded fashion was done on differential cell counts of Pappenheim-stained cytocentrifuge preparations, using overall morphologic criteria, including differences in cell size and shape of nuclei. Protein in bronchoalveolar lavage was determined according to Lowry et al (21).

Model of Intraperitoneal Inflammation. Mice were anesthetized with xylazine/ketamine, and LPS (2 μg/mouse) or vehicle was injected intraperitoneally. For cytokine measurements from plasma and white blood cell count in peripheral blood, mice were exsanguinated 2 hrs after LPS treatment in deep anesthesia.

Enzyme-Linked Immunosorbent Assay. Cytokine enzyme-linked immunosorbent assays for tumor necrosis factor (TNF)-α and macrophage inflammatory protein (MIP)-2 were performed according to the manufacturer's (R&D, Wiesbaden, Germany) instructions.

Myeloperoxidase Assay. Lung myeloperoxidase (MPO) was determined as an index of tissue neutrophil accumulation 24 hrs after LPS challenge as described (22). After weighing of lung stored at −80°C, the frozen lung was homogenized, sonicated, and centrifuged at 25,000 × *g*. MPO activity was calculated from change in absorbance (460 nm) resulting from decomposition of H_2O_2 in the presence of o-dianisidine.

Wet-to-Dry Ratio. To assess pulmonary edema, determination of lung wet weight was performed after removal of extraneous bronchial and cardiac structures as described (23). To measure dry weight, lungs were incubated in a drying oven a week at 80°C and then reweighed.

Peripheral White Blood Cell Counts. White blood count of peripheral blood was measured as previously described (24).

Experimental Protocol. Seven days after central venous catheter implantation in mice, exchange of pumps was performed. Then, 200 μL per day of either SO, FO, or 0.9% NaCl was infused over 3 days with the mice being al-

lowed access to water and chow *ad libitum*. The amount of lipids infused is equivalent to 1.0 g/kg/day. However, the energy expenditure of mice is nearly three times higher that that of humans. Therefore, the infused lipids were considered to be close to lower limits of recommended amount of lipids in parenteral nutrition. While receiving infusions, mice were subjected to low-dose unfractionated heparin injected subcutaneously. In experiments with WT mice treated with PAF-RA, 10 mg/kg of body weight BN52021 (Biomol, Hamburg, Germany) was injected into the tail vein 30 mins before intratracheal LPS application.

Statistics. Data are given as the mean ± SEM. Two-way analysis of variance was performed to test for differences between different infusion groups and mice strains (WT, PAF-R −/−, PAF-RA). *Post hoc* analysis was carried out using Student-Newman-Keuls' test. As data of protein in lavage and leukocytes in BAL (1 μg, 24 hrs) were not normally distributed, log-transformation was performed. Wet-to-dry ratios between unstimulated and stimulated groups were compared using Student's *t*-test. Probability (p) values <.05 were considered to indicate statistical significance. Analysis was carried out using SigmaStat.

RESULTS

Effect of Lipid Emulsions on Alveolar Leukocyte Recruitment and Wet-to-Dry Ratio in LPS-Induced Acute Lung Injury. Without LPS challenge, we found $0.10 \pm 0.01 \times 10^6$ leukocytes in the BAL fluid without significant variation between NaCl and lipid infusion groups. After stimulation of WT mice with 1 μg of LPS, leukocytes migrated into the alveolar space, with their numbers in BAL fluid rising to $1.09 \pm 0.08 \times 10^6$ cells after 24 hrs (Fig. 1*A*). Preinfusion of SO massively increased leukocyte recruitment by nearly 100% ($p < .01$ vs. NaCl). In contrast, in mice receiving FO, leukocytes were significantly reduced to <60% ($p < .01$ vs. SO and NaCl). When using 10

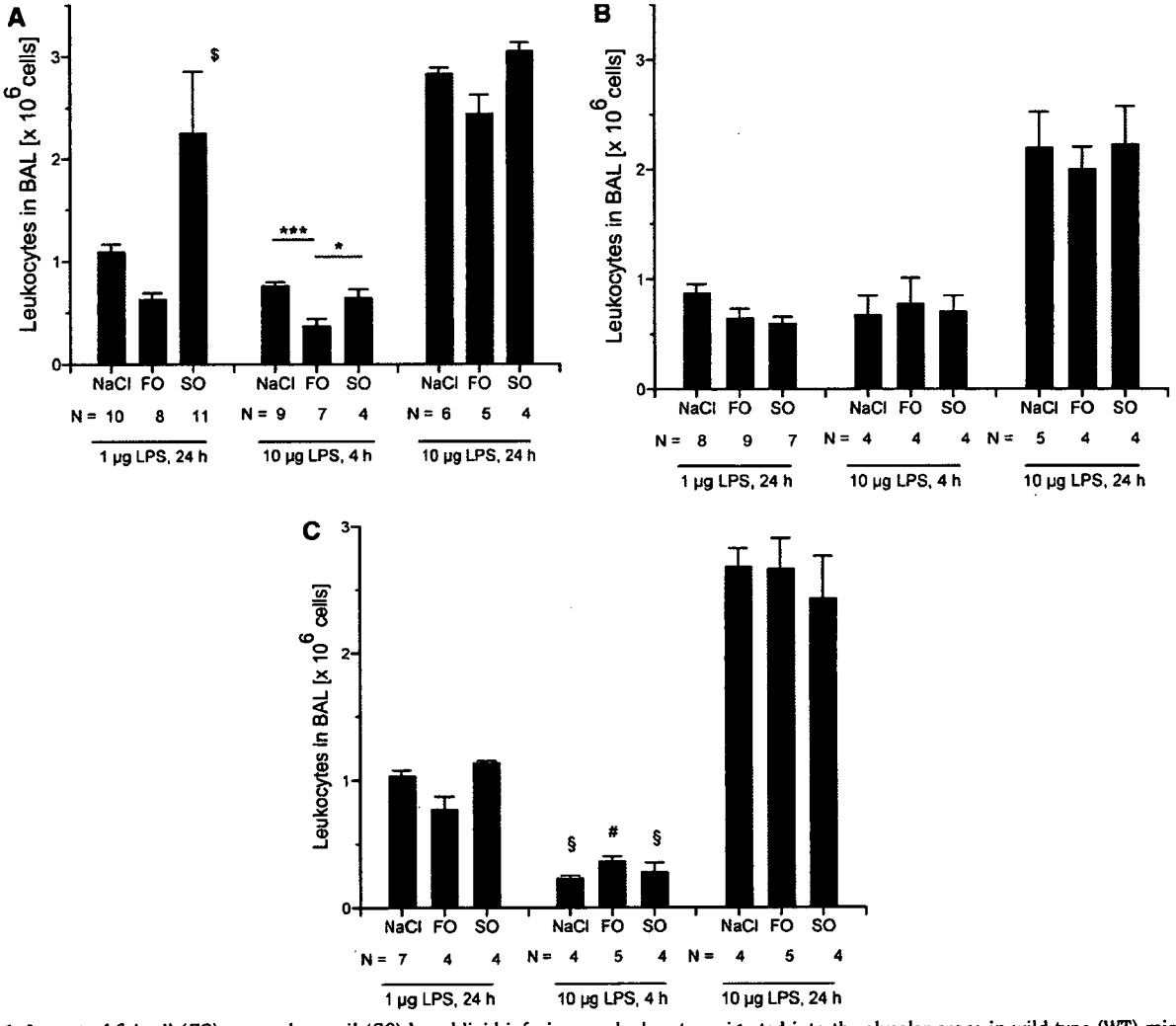

Figure 1. Impact of fish oil (*FO*)- vs. soybean oil (*SO*)-based lipid infusions on leukocytes migrated into the alveolar space in wild-type (WT) mice, mice lacking the platelet-activating factor-receptor (PAF-R −/−), and WT mice treated with platelet-activating factor receptor antagonist (PAF-RA) in a model of acute lung injury. WT mice (*A*), PAF-R −/− mice (*B*), and WT mice treated with a PAF-RA (*C*) were infused with saline (*NaCl*) or FO- or SO-based lipid emulsions, followed by application of 1 or 10 μg of endotoxin (lipopolysaccharide, LPS) intratracheally 4 or 24 hrs before performing a bronchoalveolar lavage (*BAL*). Total lavage leukocyte counts are given. Only in WT mice, a significant difference of SO- vs. FO-based lipid emulsions, and of saline (control) vs. FO-based lipid emulsion, respectively, was detectable ($\$p < .01$ all groups differed significantly from each other; $*p < .05$ FO vs. SO; $***p < .001$ FO vs. control). Animals exposed to 10 μg of LPS for 4 hrs in the PAF-RA groups exhibited a reduction of leukocyte numbers ($\S p < .05$ vs. WT and PAF-R −/−; $\#p < .05$ vs. PAF-R −/−). Data are given as mean ± SEM. Numbers of animals per group are detailed below columns. Error bars are missing when falling into symbol.

μg of LPS in the normal saline group, we found 0.76 ± 0.04 × 10^6 leukocytes after 4 hrs rising to 2.83 ± 0.06 × 10^6 leukocytes after 24 hrs in the BAL. After 4 hrs, infusion of FO-based lipid emulsions induced a significant reduction of transmigrated leukocytes by nearly 50% ($p < .001$ vs. NaCl and $p < .05$ vs. SO), whereas SO had no impact on leukocyte invasion compared with NaCl. After 24 hrs in mice receiving SO, leukocyte invasion was comparable to mice receiving NaCl, whereas infusions of FO-based lipids led to a small reduction.

Without LPS challenge, differential count of leukocytes in BAL was 2.5 ± 0.8% granulocytes, 97.0 ± 0.9% monocytes/macrophages, and 0.5 ± 0.3% lymphocytes without effect of lipid emulsions on this feature. At 24 hrs after challenge with 1 μg of LPS, 78.1 ± 3.2% granulocytes, 2.0 ± 0.4% lymphocytes, and 20.2 ± 3.1% monocytes/macrophages were detected in the BAL of WT mice receiving NaCl. This profile of predominant neutrophil invasion was not changed by infusion of lipids or LPS dose.

Wet-to-dry ratio was determined to evaluate degree of lung injury. Without LPS, wet-to-dry ratio was 4.62 ± 0.07 in control animals with both lipid infusions exhibiting no further impact. After instillation of 10 μg of LPS in mice receiving normal saline, wet-to-dry ratio increased to 5.12 ± 0.09 after 24 hrs ($p < .01$ vs. control) whereas both lipid emulsions did not modulate this feature and did not differ significantly from the NaCl group.

Significance of PAF-R for Recruitment of Leukocytes Into the Alveolar Space and Its Modulation by Lipid Emulsions. Bronchoalveolar lavage performed 4 or 24 hrs after intratracheal LPS challenge with 1 or 10 μg of LPS in PAF-R −/− mice submitted to infusion of normal saline (control) indicated a similar response as encountered in corresponding WT animals. Quantity (Fig. 1*B*) and cell differentiation of recruited leukocytes were not different in both strains. The diverging effect of preinfused lipid emulsions on alveolar recruitment of leukocytes was, however, fully lost in PAF-R −/− mice. In both lipid infusion groups, numbers of recruited leukocytes were slightly but not statistically significantly different compared with normal saline control mice. This finding was irrespective of LPS dose or time of lavage.

To confirm our results in PAF-R −/− mice, we treated WT mice with the PAF-RA BN52021. WT mice were infused for 3 days with normal saline (NaCl control) or with FO- or SO-based lipid emulsions followed by application of 1 or 10 μg/mouse LPS intratracheally 4 or 24 hrs before performing a BAL (Fig. 1*C*). A dose of 10 mg/kg BN52021 was injected into the tail vein 30 mins before LPS application. In mice treated with normal saline, the absolute leukocyte numbers and differential count in BAL did not differ from WT or PAF-R −/− mice 24 hrs after LPS challenge. However, 4 hrs after instillation of 10 μg of LPS, we found a strong reduction of leukocytes in all PAF-RA groups. The reduction was significant in animals receiving NaCl or SO compared with respective WT and PAF-R −/− groups ($p < .05$ for each comparison). In animals receiving FO, leukocytes were significantly lower compared with the FO-PAF-R −/− group ($p < .05$) but comparable to WT mice infused with FO-based emulsions.

As in PAF-R −/− mice, FO or SO no longer modulated the amount of alveolar recruited leukocytes after treatment with a PAF-RA. This was consistent irrespective of time of lavage and dose of LPS. In particular, in contrast to WT mice, SO-based lipid emulsions lost their capacity to double alveolar leukocyte transmigration.

LPS-Induced Accumulation of Neutrophils in Lung Tissue. MPO activity was measured before and 24 hrs after LPS challenge to assess neutrophil accumulation in lung tissue. In lungs of WT mice without LPS exposure, MPO activity was 0.9 ± 0.3 units/g without significant effect of lipid emulsions (Table 2). After instillation of 10 μg of LPS, MPO increased to 6.6 ± 0.7 units/g in control animals. After infusion of SO-based lipid emulsions, MPO was nearly two-fold higher compared with the FO and normal saline groups ($p < .05$ for each comparison). After application of 1 μg of LPS intratracheally, we found the same trend for MPO determination in WT animals, but results failed to reach the level of significance. The diverging effect of preinfused lipid emulsions on neutrophil accumulation in lung tissue was, however, lost in PAF-R −/− mice and after application of the PAF-RA in mice receiving 10 μg of LPS.

LPS-Induced Alveolar Protein Leakage. To examine the impact of lipids on lung injury, we determined protein in the BAL as marker for vascular leakage. In WT animals without LPS challenge, protein concentration was determined as 32 ± 3 μg/mL without significant modulation by lipid emulsions (Table 3). After intratracheal challenge with 1 μg or 10 μg of LPS, protein in BAL increased to 273 ± 16 μg/mL or 551 ± 34 μg/mL, respectively, after 24 hrs in WT animals. Infusion of FO significantly decreased alveolar protein leakage after 1 μg ($p < .01$ vs. NaCl and SO) and 10 μg of LPS, whereas after SO infusion protein concentrations slightly increased. Due to the marked reduction of protein in BAL after FO after 1 μg of LPS, FO-WT animals differed significantly from FO-PAF-R −/− mice ($p < .05$).

Generation of MIP-2 After LPS Instillation. We then examined the impact of lipid emulsions on intra-alveolar cytokine generation in our model. Without LPS stimulation, MIP-2 concentration in BAL

Table 2. Myeloperoxidase activity in lung homogenates (units/g of tissue)

	Without LPS	1 μg of LPS (24 Hrs)	10 μg of LPS (24 Hrs)
Wild-type			
NaCl	0.9 ± 0.3 (n = 4)	3.3 ± 0.7 (n = 4)	6.6 ± 0.7 (n = 8)
FO	1.0 ± 0.4 (n = 4)	3.4 ± 0.4 (n = 4)	6.8 ± 1.4 (n = 4)
SO	0.9 ± 0.4 (n = 4)	5.1 ± 0.9 (n = 4)	11.3 ± 0.9 (n = 4)[a]
PAF-R −/−			
NaCl	0.8 ± 0.4 (n = 4)	ND	9.1 ± 1.0 (n = 4)
FO	0.9 ± 0.4 (n = 4)	ND	9.4 ± 1.4 (n = 4)
SO	0.9 ± 0.3 (n = 4)	ND	7.7 ± 0.5 (n = 4)
PAF-RA			
NaCl	0.9 ± 0.4 (n = 4)	ND	9.5 ± 1.5 (n = 4)
FO	0.8 ± 0.4 (n = 4)	ND	8.3 ± 0.4 (n = 4)
SO	0.9 ± 0.5 (n = 4)	ND	9.6 ± 1.6 (n = 4)

LPS, lipopolysaccharide; NaCl, saline; FO, fish oil; SO, soybean oil; PAF-R −/−, mice lacking the platelet-activating factor receptor; ND, not done; PAF-RA, platelet-activating factor receptor antagonist.

[a]$p < .05$ for comparison with NaCl and FO. Wild-type mice, PAF-R −/− mice, and wild-type mice treated with a PAF-RA were infused for 3 days with NaCl (control) or with FO- or SO-based lipid emulsions, followed by stimulation with 1 or 10 μg of endotoxin (LPS) intratracheally for 24 hrs.

Table 3. Protein concentration in bronchoalveolar lavage (μg/mL)

	Without LPS	1 μg of LPS (24 Hrs)	10 μg of LPS (24 Hrs)
Wild-type			
NaCl	32 ± 3 (n = 4)	273 ± 16 (n = 21)	551 ± 34 (n = 4)
FO	33 ± 4 (n = 4)	148 ± 21 (n = 6)[a,b]	416 ± 21 (n = 5)[c]
SO	31 ± 5 (n = 5)	313 ± 40 (n = 11)	641 ± 11 (n = 4)
PAF-R −/−			
NaCl	31 ± 4 (n = 4)	347 ± 36 (n = 11)	382 ± 89 (n = 6)
FO	33 ± 5 (n = 4)	338 ± 69 (n = 9)	462 ± 43 (n = 4)
SO	32 ± 5 (n = 4)	304 ± 67 (n = 7)	654 ± 115 (n = 5)
PAF-RA			
NaCl	33 ± 4 (n = 4)	325 ± 40 (n = 4)	552 ± 86 (n = 4)
FO	33 ± 3 (n = 4)	253 ± 50 (n = 4)	424 ± 102 (n = 6)
SO	32 ± 4 (n = 4)	331 ± 70 (n = 4)	527 ± 119 (n = 6)

LPS, lipopolysaccharide; NaCl, saline; FO, fish oil; SO, soybean oil; PAF-R −/−, mice lacking the platelet-activating factor receptor; PAF-RA, platelet-activating factor receptor antagonist.

[a]Within WT, $p < .01$ FO vs. NaCl and SO; [b]within FO infusion groups, $p < .05$ WT vs. PAF-R−/−; [c]within WT, $p < .05$ FO vs. SO. Wild-type mice (WT), PAF-R −/− mice, and WT mice treated with a PAF-RA were infused for 3 days with NaCl (control) or with FO-, or SO-based lipid emulsions, followed by stimulation with 1 or 10 μg of endotoxin (LPS) intratracheally for 24 hrs.

was below detection limit regardless of infusion used or mouse line examined. At 24 hrs after challenge with 1 μg of LPS, we found an increase in lavage MIP-2 concentration to 112 ± 6 pg/mL in mice infused with normal saline (Fig. 2*A*). In mice receiving SO, MIP-2 was similar compared with the NaCl group. However, in mice receiving FO, MIP-2 concentration was significantly reduced ($p < .001$ vs. NaCl and $p < .05$ vs. SO). When using 10 μg of LPS in the normal saline group, we found a tremendous increase in MIP-2 after 4 hrs to 1225 ± 96 pg/mL and a decline to 165 ± 18 pg/mL after 24 hrs. After 4 hrs, infusion of FO-based lipid emulsions induced a small reduction of MIP-2, but preinfusion with SO provoked a significant increase of nearly 25% compared with the NaCl group ($p < .05$ vs. FO or NaCl). After 24 hrs in mice receiving SO, MIP-2 concentration remained massively elevated (741 ± 73 pg/mL, $p < .001$ vs. NaCL or FO) and was reduced to 140 ± 18 pg/mL in the FO group.

In PAF-R −/− mice receiving normal saline, MIP-2 levels 24 hrs after challenge with 1 or 10 μg of LPS were comparable to WT animals. The MIP-2 concentrations in both lipid infusion groups did not differ significantly from each other and from saline control irrespective of time of lavage or dose of LPS (Fig. 2*B*). After 4 hrs in mice receiving 10 μg of LPS, MIP-2 concentrations were significantly higher compared with corresponding WT animals in the NaCl and FO groups ($p < .05$) but did not differ from the animals receiving SO.

To confirm our results in PAF-R −/− mice, we treated WT mice with the PAF-RA BN52021. At 24 hrs after challenge with 1 μg of LPS, PAF-RA pretreatment exhibited a reduction of MIP-2 down to about one third compared with WT and PAF-R −/− mice receiving normal saline (Fig. 2*C*, $p < .05$). This reduction by PAF-RA pretreatment was also found in mice receiving either lipid emulsion compared with WT and PAF-R −/− animals ($p < .05$).

Using 10 μg of LPS in the PAF-RA group, MIP-2 concentrations after 4 and 24 hrs were similar to the concentrations detected in WT and PAF-R −/− mice receiving NaCl. In contrast to WT animals, but similar to PAF-R −/−, application of PAF-RA abolished differential impact of FO vs. SO lipid infusions on intra-alveolar MIP-2 concentrations irrespective of dose of LPS or time of lavage. Due to the massive increase after infusion of SO-based lipid emulsions, WT animals differed significantly from PAF-R −/− and PAF-RA groups ($p < .01$).

TNF-α Concentration in BAL After LPS Challenge. Next, we examined impact of lipid emulsions on TNF-α concentration in BAL. Without LPS stimulation, TNF-α was undetectable in BAL in all groups irrespective of mouse line and infusion used. At 24 hrs after challenge with 1 μg of LPS, we found an increase in TNF-α concentration to 162 ± 12 pg/mL in mice infused with normal saline (Fig. 3*A*). In mice receiving SO, a similar TNF-α concentration was detected. In contrast, infusion of FO resulted in a significant reduction of TNF-α ($p < .05$ vs. NaCl and SO). After challenge with 10 μg of LPS in mice receiving normal saline, TNF-α concentration massively rose to 1496 ± 92 pg/mL after 4 hrs and to 564 ± 126 pg/mL after 24 hrs. After 4 hrs, infusion of SO led to a further small increase. In contrast, in the FO group, TNF-α was significantly reduced by nearly 25% compared with the NaCL group ($p < .05$ vs. NaCl and SO). However, in the BAL performed after 24 hrs, TNF-α concentration was not significantly modulated by lipid emulsions.

In PAF-R −/− mice receiving NaCl infusions, TNF-α was slightly lower after LPS challenge as compared with WT animals (Fig. 3*B*). TNF-α concentrations in the FO or SO group did not differ significantly from each other and from saline control irrespective of time of lavage or dose of LPS.

To confirm our results in PAF-R −/− mice, we treated WT mice with the PAF-RA BN52021. At 24 hrs after challenge with 1 μg of LPS, TNF-α concentration in PAF-RA-pretreated mice receiving NaCl was 100 ± 12 pg/mL, exhibiting a significant reduction by nearly 40% compared with saline-infused WT mice ($p < .05$, Fig. 3*C*). When instilling 10 μg of LPS, TNF-α concentrations after 4 and 24 hrs were similar to concentrations determined in WT and PAF-R −/− mice receiving normal saline. In contrast to WT animals, but similar to PAF-R −/−, injection of PAF-RA inhibited the differential impact of FO and SO lipid infusions on intra-alveolar TNF-α concentrations irrespective of dose of LPS or time of lavage.

After 4 hrs in mice stimulated with 10 μg of LPS, TNF-α concentrations were increased in all infusion groups receiving PAF-RA. In mice infused with FO, the PAF-RA mice differed significantly from the WT and PAF-R −/− animals ($p < .05$). As TNF-α was also increased in WT mice after SO infusion, the PAF-RA SO group and the WT SO group differed significantly from the PAF-R −/− mice ($p < .05$).

Cytokine Concentrations in Plasma After Intraperitoneal LPS Instillation. Next, we asked if lipid emulsions would have similar effects in a model of abdominal inflammation. In pilot experiments, we determined that TNF-α concentration in plasma peaked at 2 hrs after intra-abdominal LPS instillation in our model. Using the previous infusion setting, we challenged mice with 2 μg LPS intraperitoneally 2 hrs before kill and bleeding.

Before LPS challenge, leukocyte counts in peripheral blood were 6.6 ± 0.4 G/L